4,4-Difluoroproline as a Unique ^{19}F NMR Probe of Proline Conformation

Himal K. Ganguly, Brice A. Ludwig, Caitlin M. Tressler, Megh R. Bhatt, Anil K. Pandey, Caitlin M. Quinn, Shi Bai, Glenn P. A. Yap, and Neal J. Zondlo*

Department of Chemistry and Biochemistry

University of Delaware

Newark, DE 19716

United States

* To whom correspondence should be addressed. email: *zondlo@udel.edu*, phone: +1-302-831-0197.

Abstract

Despite the importance of proline conformational equilibria (*trans* versus *cis* amide, *exo* versus *endo* ring pucker) on protein structure and function, there is a lack of convenient ways to probe proline conformation. 4,4-Difluoroproline (Dfp) was identified to be a sensitive ^{19}F NMR-based probe of proline conformational biases and of *cis-trans* isomerism. Within model compounds and disordered peptides, the diastereotopic fluorines of Dfp exhibit similar chemical shifts ($\Delta\delta_{FF}$ = 0–3 ppm) when a *trans* X–Dfp amide bond is present. In contrast, the diastereotopic fluorines exhibit a large ($\Delta\delta_{FF}$ = 5–12 ppm) difference in chemical shift in a *cis* X–Dfp prolyl amide bond. DFT calculations, X-ray crystallography, and solid-state NMR spectroscopy indicated that the $\Delta\delta_{FF}$ directly reports on the relative preference of one proline ring pucker over the other: a fluorine which is pseudo-axial (i.e. the *pro*-4*R*-F in an *exo* ring pucker, or the *pro*-4*S*-F in an *endo* ring pucker) is downfield, while a fluorine which is pseudo-equatorial (i.e. *pro*-4*S*-F when *exo*, or *pro*-4*R*-F when *endo*) is upfield. Thus, when a proline is disordered (a mixture of *exo* and *endo* ring puckers, as at *trans*-Pro in peptides in water), it exhibits a small $\Delta\delta$. In contrast, when the Pro is ordered (i.e. when one ring pucker is strongly preferred, as in *cis*-Pro amide bonds, where the *endo* ring pucker is strongly favored), a large $\Delta\delta$ is observed. Dfp can be used to identify inherent induced order in peptides and to quantify proline *cis-trans* isomerism. Using Dfp, we discovered that the stable polyproline II helix (PPII) formed in the denatured state (8 M urea) exhibits essentially equal populations of the *exo* and *endo* proline ring puckers. In addition, the data with Dfp suggested the specific stabilization of PPII by water over other polar solvents. These data strongly support the importance of carbonyl solvation and $n\rightarrow\pi^*$ interactions for the stabilization of PPII. Dfp was also employed to quantify proline *cis-trans* isomerism as a function of phosphorylation and the R406W mutation in peptides derived from the intrinsically disordered protein *tau*. Dfp is minimally sterically disruptive and can be incorporated in expressed proteins, suggesting its broad application in understanding proline *cis-trans* isomerization, protein folding, and local order in intrinsically disordered proteins.

Introduction

Proline exhibits two key conformational equilibria: *trans* versus *cis* amide bond isomerism at the ω torsion angle, and the *exo* versus *endo* pyrrolidine ring pucker (Figure 1). Proline ring pucker correlates with main chain conformation, with the *exo* ring pucker promoting more compact values of ϕ and ψ and the *endo* ring pucker associated with more extended values. Proline *cis-trans* isomerization is often a rate-limiting step in protein folding, can function as a molecular timer, and has been implied to have a role in some protein misfolding diseases (e.g. the role of the phosphorylation-dependent prolyl isomerase Pin1 in tau aggregation in Alzheimer's disease).[1-5] Thus, the development of new approaches to rapidly and site-specifically identify *cis* versus *trans* proline amide bonds in solution could have broad applications in understanding protein folding and structure.

Proline *cis-trans* isomerism is typically identified by the presence of an extra set of resonances in ^{1}H NMR spectroscopy (or sets of resonances, if multiple prolines are present). However, within globular proteins, only a single proline amide conformation is typically[6] observed, so the number of resonances does not provide insights into the identity of the proline amide rotameric state. Residue-specific information on the identity of proline *cis* versus *trans* amide bond conformation can be provided by ^{13}C NMR chemical shifts (δ): in proline residues with *trans* amide bonds, the ^{13}C chemical shifts (δ) of Cβ and Cγ are similar ($\Delta\delta_{\beta\gamma}$ typically 1-4 ppm), whereas in *cis* proline amide bonds, these chemical shifts exhibit greater dispersion ($\Delta\delta_{\beta\gamma}$ 5-10 ppm).[7-10] Indeed, in the absence of X-ray crystallography, the $\Delta\delta_{\beta\gamma}$ is the best-resolved indicator of *cis* versus *trans* amide bond rotameric state in larger proteins, and can be directly observed from ^{1}H-^{13}C HSQC spectra. The alternative observation of interresidue NOEs between

Hα of the residue before proline and either Pro Hα (in *cis* amide bonds) or Pro Hδ (in *trans* amide bonds) can become problematic due to spectral overlap with other proline resonances or with the water resonance, in addition to requiring assignment of all key resonances. The problem of spectral overlap is particularly severe in proline-rich sequences or in intrinsically disordered regions of proteins, where each residue typically exhibits similar chemical shifts and where standard sequential residue assignment (via NOEs between an amide hydrogen and the Hα of the prior residue) breaks down.

The challenge of identification of amide bond rotameric state is not unique to NMR spectroscopy. Indeed, surveys of the PDB have found that *cis* amide bonds are commonly misidentified as *trans* amide bonds in lower resolution structures (especially > 2 Å), with the percentage of proline amides in a *cis* conformation observed to be greater in higher-resolution structures than in lower-resolution structures.[11,12]

We previously described a method (termed proline editing) for the site-specific modification of proline residues within peptides.[13-15] Proline editing allows the modification within peptides of a 4*R*-hydroxyproline residue to any of a series of 4-substituted prolines. One amino acid synthesized via proline editing was 4,4-difluoroproline (Dfp) (Figure 1b).[16] Moroder and others have demonstrated that 4,4-difluoroproline exhibits conformational preferences similar to those of proline (i.e. a minimal effect of Dfp compared to Pro on *exo*/*endo* ring pucker or *trans*/*cis* amide conformational equilibria in peptides).[13,15,17-22] 4,4-Difluoroproline can also be incorporated in expressed proteins via proline auxotrophic bacteria.[17,23-26] In the course of our work on proline editing, we examined the ^{19}F NMR spectra of the peptides Ac-TYDfpN-NH_2 and Ac-TADfpN-NH_2 (Figure 12 of ref. [15]). In the *trans* amide conformation, both diastereotopic fluorines exhibited similar chemical shifts ($\Delta\delta_{FF}$ = 0 to 1.3 ppm); indeed, in the peptide Ac-

TYDfpN-NH_2, only a single peak was observed, due to $\Delta\delta_{FF} < {}^2J_{FF}$. In contrast, in the *cis* amide conformation of both peptides, a large chemical shift dispersion of the fluorines was observed ($\Delta\delta_{FF} \sim$ 8–10 ppm). Raines observed similar ^{19}F NMR data for Ac-Dfp-OMe in $CDCl_3$ and in D_2O ($\Delta\delta_{FF}$ (*trans*) 0.4–4.0 ppm, $\Delta\delta_{FF}$ (*cis*) = 4.6–8.5 ppm).[18] These data suggested the possibility of using 4,4-difluoroproline as a probe of proline *cis-trans* isomerization in proteins, analogous to using $\Delta\delta_{\beta\gamma}$, but with the greater sensitivity and simplified spectra of ^{19}F NMR compared to ^{13}C NMR.[27-35]

In related work, Hilvert and coworkers described the use of a site-specifically incorporated Dfp residue to probe the mechanism of protein misfolding and amyloid formation in β2-microglobulin. In this work, they focused on the use of Dfp to reduce the activation barrier for proline *cis-trans* isomerization.[36] However, by ^{19}F NMR spectroscopy, both in peptides and within the protein, in both the folded and the denatured states, they observed proline rotamer-dependent chemical shift differences between diastereotopic fluorines ($\Delta\delta_{FF}$ = 4–14 ppm in *cis* amides, $\Delta\delta_{FF}$ < 1 ppm in *trans* amides). Collectively, these results suggested the ready distinction between *cis* and *trans* amide bonds via 4,4-difluoroproline. Therefore, we sought to more generally examine the utility of Dfp as a conformational probe, via the site-specific incorporation of 4,4-difluoroproline into a series of model compounds and peptides.

Results

Synthesis of model compounds and peptides containing 4,4-difluoroproline. In order to test the applicability of Dfp as a conformational probe, a series of distinct model compounds and peptide contexts was considered (Figure 2). Dfp was examined within the simple model compounds Ac-Dfp-OMe and Piv-Dfp-OMe (Piv = pivaloyl). The pivaloyl group was employed

based on our prior work to understand the role of $n \rightarrow \pi^*$ interactions on conformation using X–Hyp(4-NO_2-Bz)-OMe (X = acyl capping group) compounds. There, we found a significant increase in order using pivaloyl capping groups, including a stronger $n \rightarrow \pi^*$ interaction and strong promotion of PPII and of the *trans*-proline amide conformation.[37,38] In addition, we also examined peptides in which we have previously explored the impact of residue identity on proline *cis-trans* isomerism using ^{1}H NMR spectroscopy, in order to compare the results obtained via ^{1}H NMR spectroscopy versus via ^{19}F NMR spectroscopy with Dfp. Peptides examined included Ac-TY*Prox*N-NH_2 (*Prox* = 4-substituted proline) model peptides previously used to understand the roles of aromatic residues and of 4-substituted prolines on proline *cis-trans* isomerism.[13,15,39,40] Dfp was also placed within the Ac-GPP**X**PPGY-NH_2 host-guest peptide model system context used previously to characterize the PPII propensities of guest residues (including all 20 encoded amino acids) at position **X**.[41-45]

Finally, we examined the use of Dfp to quantify proline *cis-trans* isomerism in the context of a peptide derived from an intrinsically disordered protein. In the microtubule-binding protein *tau*, phosphorylation states (e.g. phosphorylation at Ser404) and mutations (R406W) in the *tau* C-terminal domain are associated with increased neurodegeneration in Alzheimer's disease and other neurodegenerative disorders.[46-53] In peptides derived from *tau*, we recently demonstrated that both Ser404 phosphorylation and the R406W modification lead to an increased population of *cis*-proline at Pro405.[54] Therefore, we examined Dfp at this position in peptides derived from residues 403-406 of *tau*, in order to understand the roles of both Ser404 phosphorylation and the R406W modification on proline *cis-trans* isomerism.

X-ray crystallography of Fmoc-Dfp-OH. In order to incorporate Dfp into peptides by solid-phase peptide synthesis, commercially available Boc-4,4-difluoroproline **1** was converted

to Fmoc-4,4-difluoroproline **3** as previously described (Figure 3a).[16] **3** crystallized from $CDCl_3$. The crystal structure of **3** (Figure 3b) exhibited a compact value of ϕ but an extended value of ψ (ϕ = –59°, ψ = +175°), a *trans* amide bond (ω = +171°), and a Cγ–*exo* ring pucker (χ_2 = +31°). The value of ψ observed is notably larger than is typical for a proline *exo* ring pucker.[55,56] In the crystal assembly, a close intermolecular hydrogen bond was observed between the carboxylic acid hydrogen and the carbamate carbonyl oxygen of an adjacent molecule (O•••H distance 1.71 Å) (Figure 3c). Only a weak $n\rightarrow\pi^*$ interaction, with poor interaction geometry, was observed between consecutive carbonyls (O•••C=O distance 3.02 Å, $\angle_{OCO}$ = 77° (ideal 109°)). Interestingly, the difluoroproline carbonyl exhibited a close C–H/O interaction[12,57-61] with chloroform (H•••O distance 2.25 Å) (Figure 3b), as well as a C–H/O interaction (2.60 Å) between one ProHβ and the carbamate carbonyl (Figure 3d). These observations are consistent with our recent report that C–H/O interactions are a general mode for structure stabilization and molecular assembly at proline residues.[62]

^{19}F NMR spectroscopy of 4,4-difluoroproline in model compounds and model peptides. The previously reported ^{1}H-coupled ^{19}F NMR spectrum of Ac-TYDfpN-NH_2 in water (5 mM phosphate buffer, 25 mM NaCl, pH 4) revealed that, in the *cis* amide conformation, the diastereotopic fluorines exhibited highly divergent ^{19}F chemical shifts (Figure 4).[15] Each diastereotopic fluorine in the *cis*-proline conformation appears as a doublet due to coupling between the geminal fluorines ($^2J_{FF}$ = 236 Hz) (Figure 4d). In contrast, for *trans*-proline, because the chemical shift difference between the fluorines is less than their coupling constant ($\Delta\delta < {}^2J_{FF}$), the fluorines become magnetically equivalent and appear as a singlet in the ^{19}F NMR spectrum.

In order to understand the basis for the observed ^{19}F chemical shifts, we examined the ^{1}H-coupled ^{19}F NMR spectra (Figure 4e). The ^{19}F resonances in *cis*-proline exhibited distinct $^{3}J_{HF}$ coupling patterns of the fluorines to the β and δ hydrogens. When a fluorine in Dfp is pseudo-axial (i.e. the *pro*-4*S*-fluorine in an *endo* ring pucker, or the *pro*-4*R* fluorine in an *exo* ring pucker), the fluorine is nearly *anti*-periplanar to one Hβ and to one Hδ (Figure 4b), and thus should exhibit larger coupling constants with these two vicinal hydrogens. In contrast, when a fluorine in Dfp is pseudo-equatorial (i.e. the *pro*-4*R*-fluorine in an *endo* ring pucker, or the *pro*-4*S* fluorine in an *exo* ring pucker), the fluorine is approximately *gauche* to all vicinal hydrogens, and thus should exhibit only smaller $^{3}J_{HF}$ coupling constants.

The *endo* and *exo* proline ring puckers are in rapid equilibrium due to a small activation barrier ($\Delta G^{\ddagger} \sim 2$ kcal mol^{-1}) for interconversion, with each diastereotopic fluorine being pseudo-axial in one ring pucker and pseudo-equatorial in the other ring pucker. Therefore, in a typical disordered conformation, with similar populations of *endo* and *exo* ring puckers,[55,63-66] both diastereotopic fluorines should exhibit similar patterns of $^{3}J_{HF}$ coupling, due to the observed $^{3}J_{HF}$ representing the population-weighted average of the two ring puckers. Indeed, here for *trans*-proline, the coupling pattern appears as a quintet, indicating similar $^{3}J_{HF}$ of each fluorine with each of the 4 vicinal Hβ and Hδ.

In contrast, if one ring pucker is significantly preferred, then the fluorines should exhibit distinct chemical shifts and patterns of coupling constants, corresponding to those of the major ring pucker present in solution. Proline predominantly adopts an *endo* ring pucker when in the *cis* amide conformation.[55,56,64] Based on the different patterns of the coupling constants in the fluorines (larger apparent $^{3}J_{HF}$ coupling constants observed at the downfield fluorine, but all smaller apparent $^{3}J_{HF}$ values at the upfield fluorine), the downfield fluorine resonance (δ = –95.0

ppm) in this peptide in water was assigned as the *pro*-4*S* fluorine. In an *endo* conformation (Figure 4b), the *pro*-4*S* fluorine is nearly *anti*-periplanar to one Hβ and to one Hδ, and thus should exhibit larger coupling constants ($^3J_{HF}$ over 30 Hz has been observed for strong hyperconjugative interactions[67]) (Figure 4c). In contrast, the *pro*-4*R* fluorine in the *endo* ring pucker would be approximately *gauche* to all Hβ and Hδ, and thus should exhibit smaller overall coupling constants. A similar pattern was previously seen in the ^{1}H-coupled ^{19}F NMR spectrum of Ac-Dfp-OMe.[18] These results suggested that the downfield ^{19}F resonance might be associated with a [predominantly] pseudo-axial fluorine, while the upfield ^{19}F resonance might be associated with a [predominantly] pseudo-equatorial fluorine.

We emphasize that proline *cis* and *trans* amide rotamers are in slow exchange on the NMR timescale ($\Delta G^{\ddagger} \sim 20$ kcal mol^{-1}), and thus the resonances associated with the *trans*-proline and *cis*-proline conformations are distinct. In contrast, the interconversion between the *endo* and *exo* ring puckers ($\Delta G^{\ddagger} \sim 2$ kcal mol^{-1}) is rapid (conformers in fast exchange) on the NMR timescale, and thus the proline ring puckers are not observed as distinct resonances by NMR spectroscopy. Instead, the NMR spectrum represents the *population-weighted average* of the ^{19}F chemical shifts and coupling constants of a fluorine in *both* the *endo* and *exo* ring puckers.

The model compounds Ac-Dfp-OMe and Piv-Dfp-OMe were similarly examined by ^{19}F NMR spectroscopy as a function of solvent, in deuterated methanol, acetonitrile, and chloroform (Figure 5). In all solvents, Ac-Dfp-OMe exhibited an equilibrium between the *trans*-proline and *cis*-proline rotamers, with a higher population of *trans*-proline in all solvents (Figure 5c).[17,18] In all cases, by ^{19}F NMR, the *cis*-proline rotamer exhibited a larger chemical shift difference between the diastereotopic fluorines than was observed for *trans*-proline. For Piv-Dfp-OMe, only the *trans*-proline rotamer was observed (Figure 5d), as expected based on prior results.[37,38]

The patterns of chemical shift differences between the diastereotopic fluorines in Piv-Dfp-OMe ($\Delta\delta_{FF}$ = 0–3.1 ppm) were similar to those observed for *trans*-proline in Ac-Dfp-OMe ($\Delta\delta_{FF}$ = 1.1–2.4 ppm), and significantly smaller than those of Ac-Dfp-OMe with the *cis*-proline rotamer ($\Delta\delta_{FF}$ = 4.6–7.5 ppm).

The ^{1}H-coupled ^{19}F NMR spectra of Ac-Dfp-OMe (Figure 5e) exhibited similar patterns of $^{3}J_{HF}$ coupling constants as were observed for Ac-TYDfpN-NH_2: the downfield fluorine exhibited overall larger apparent $^{3}J_{HF}$, while the upfield fluorine exhibited smaller apparent coupling constants. These results suggested that the fluorine with a downfield ^{19}F resonance was predominantly pseudo-axial, while the upfield ^{19}F resonance was predominantly pseudo-equatorial, with a large chemical shift difference between the fluorines indicating a strong bias toward one ring pucker (as is present for *cis*-proline and the *endo* ring pucker), while a small chemical shift difference indicates a weak preference for one ring pucker (as is observed for *trans*-proline in water).[55,64,65]

Calculations on 4,4-difluoroproline in model compounds. In order to further understand the relationships between proline ring pucker, proline main-chain (ϕ,ψ) conformation, proline amide (ω) rotamer, and ^{19}F chemical shift, we conducted DFT calculations on Ac-Dfp-OMe and Ac-Piv-OMe (Figure 6).[68,69] All conformers were subjected to full geometry optimization, followed by analysis of the calculated chemical shifts as a function of conformation. These results were unequivocal: in all conformations in both molecules, the pseudo-axial fluorine (*pro*-4*R* in an *exo* ring pucker, *pro*-4*S* in an *endo* ring pucker) was downfield, and the pseudo-equatorial fluorine (*pro*-4*S* in an *exo* ring pucker, *pro*-4*R* in an *endo* ring pucker) was upfield. The chemical shift differences between the diastereotopic fluorines in any individual conformation of Ac-Dfp-OMe were 9.5–20 ppm, depending on the main-chain conformation.

Similar results were observed in implicit water and in implicit chloroform, indicating that the effect of conformation on ^{19}F chemical shift has minimal solvent dependence, and thus should be general in different contexts (e.g. a solvent-exposed proline versus a proline buried in a protein hydrophobic core). The same general results were also observed for Piv-Dfp-OMe. In addition, the *endo* ring pucker was also observed with relatively more downfield chemical shifts for the pseudo-axial fluorine, although these effects were smaller than the effect of being pseudo-axial versus pseudo-equatorial. Similar results were also observed for the model compounds with C-terminal amides Ac-Dfp-NMe_2 and Piv-Dfp-NMe_2; see the Supporting Information for details.

The calculations suggested that the basis for the chemical shift difference of the fluorines is likely directly related to the inherent stereoelectronic effects that stabilize fluorines when pseudo-axial.[67,70] These effects are analogous to the stereoelectronic effects that stabilize alcohols in the axial position (α anomer) at the anomeric carbon in carbohydrates.[71,72] When a fluorine is pseudo-axial, it is stabilized by hyperconjugative interactions between the electron-accepting C–F antibonding orbital (σ^*_{C-F}) and an electron-donating C–H bonding orbital (σ_{C-H}) and to which it is approximately *anti*-periplanar. Stabilization occurs via hyperconjugation of σ^*_{C-F} with both C–Hβ and C–Hδ (which results in a *syn*-periplanar [overlapping orbitals] relationship of σ^*_{C-F} with each σ_{C-H}). Electron delocalization between these C–H σ bonding orbitals and the C–F σ* antibonding orbital (overlap of the σ_{C-H} with the σ^*_{C-F}, a $\sigma \rightarrow \sigma^*$ interaction) is stabilizing. This electron delocalization also results in a longer C–F bond for the pseudo-axial C–F than the pseudo-equatorial C–F, as was seen computationally and is observed more generally for hyperconjugation.[73]

Solid-state NMR spectroscopy of crystalline Fmoc-Dfp-OH. These computational results suggested that, in any molecule with a strong bias for one proline ring pucker, Dfp substitution

for Pro should result in a large chemical shift difference between the diastereotopic fluorines. In the X-ray crystal structure of Fmoc-Dfp-OH (Figure 3), Dfp was observed to adopt an *exo* ring pucker, and therefore should exhibit a large difference between the chemical shifts of its fluorines. Therefore, we examined the crystals of Fmoc-Dfp-OH by solid-state ^{19}F NMR spectroscopy, as a function of spinning rate by magic angle spinning (MAS).[74-76] The solid-state ^{19}F NMR spectrum (Figure 7) indicated two central-band resonances, associated with the two diastereotopic fluorines. The observed 12.5 ppm chemical shift difference between the fluorines was very similar to the calculated 11.0 ppm chemical shift difference between the diastereotopic fluorines for Ac-Dfp-OMe in the crystallographically observed conformation (*exo* ring pucker and PPII conformation). In addition, calculations on Fmoc-Dfp-OH•$CHCl_3$ and the computationally simpler molecule EtOC(O)-Dfp-OH•$CHCl_3$, with the geometry of each restrained to that observed crystallographically, were consistent with the solid-state NMR data, with the pseudo-axial *pro*-4*R* fluorine downfield and the pseudo-equatorial *pro*-4*S* fluorine upfield, and a 12–14 ppm chemical shift difference between those fluorines, similar to that observed by solid-state MAS NMR; see the Supporting Information for details.

Temperature-dependent ^{19}F NMR spectra of model compounds. Overall, the calculations indicated that observed chemical shift differences between the diastereotopic fluorines of Dfp reflect the inherent preferences at a given residue for one proline ring pucker over the other. As the energy differences between the proline ring puckers are small in most contexts, the effects of these energy differences on the populations of the *exo* versus *endo* ring puckers should be manifested as a function of temperature. At lower temperatures, a larger population of the lower-energy ring pucker versus the higher-energy ring pucker should be observed (as $\Delta G = -RT \ln K_{exo/endo}$), which would be manifested as a larger chemical shift difference between the fluorines

at lower temperature. This analysis assumes only small enthalpic effects on the stability of one ring pucker versus the other. Therefore, we examined the ^{19}F NMR spectra of Ac-Dfp-OMe and Piv-Dfp-OMe as a function of temperature (Figure 8, Table 1).

For Ac-Dfp-OMe in methanol and acetonitrile, larger chemical shift differences between the diastereotopic fluorines were observed at lower temperatures, in both the *cis*-proline and *trans*-proline rotamers. These results are consistent with higher populations of the lowest-energy ring pucker at lower temperatures. In chloroform, this observation was also observed for *cis*-proline. In contrast, for *trans*-proline, the data indicated that the *endo* and *exo* ring puckers became equienergeic at lower temperatures, based on the observation of only a single peak for *trans*-Dfp at ≤ 243 K. For Piv-Dfp-OMe, the temperature-dependent ^{19}F NMR data indicated the possibility of a change in the main-chain conformation, as suggested by the more upfield ^{19}F chemical shifts at lower temperature.

Notably, at lower temperatures the *cis*-proline rotamer of Piv-Dfp-OMe was also observed as a very minor species (~2–3% of the total population) by ^{19}F NMR (Figure 8cd). The *pro*-4*S* fluorine δ was particularly downfield, with a large Δδ observed for *cis*-proline in all solvents. Calculations on Piv-Dfp-OMe indicated that the *exo* ring pucker is particularly disfavored for *cis*-Dfp, with the pivaloyl acyl group ≥ 2 kcal mol^{-1} higher energy for either *cis*–*exo* conformer than either *cis*–*endo* conformer. In addition, the calculated ^{19}F chemical shifts for Piv-*cis*-Dfp-OMe with an *endo* ring pucker were the most downfield chemical shifts identified computationally, as was also observed experimentally. Finally, the ^{19}F NMR spectra permitted the identification of this very low population of *cis*-proline, which could not be definitively identified in the equivalent ^{1}H NMR spectra. These data emphasize the advantages of the simplified ^{19}F spectra in the identification of minor *cis*-proline species in solution.

Understanding the effects of solvation and urea on the stabilization of PPII. The polyproline II helix (PPII) conformation has been proposed to be stabilized by solvation with water, although other bases for PPII stability have alternatively been proposed.[77-81] In order to better understand the role of solvation in stabilization of PPII, the peptide Ac-GPPDfpPPGY-NH_2 was examined by circular dichroism in water and in acetonitrile (Figure 9). In water, this peptide exhibited a somewhat reduced magnitude of mean residue ellipticity at 228 nm compared to the peptide with proline at the central (guest) residue.[41-45] These data indicate that Dfp strongly supports PPII, although it modestly destabilizes PPII relative to proline. These results are consistent with the somewhat greater likelihood of Dfp to induce *cis* amide bonds compared to proline in the model peptides Ac-Dfp-OMe or Ac-TADfpN-NH_2, as well as with a somewhat weaker $n\rightarrow\pi^*$ interaction for Dfp compared to proline.[13,15,17,18,82] In acetonitrile, Ac-GPPDfpPPGY-NH_2 also exhibited a significant, though smaller, PPII CD signature.

Urea strongly promotes PPII, which has led to proposals that PPII is a major conformation in the denatured states of proteins.[77,81,83-85] The CD spectrum of this peptide in 8 M urea exhibited a much stronger CD signature of PPII, consistent with prior data that urea promotes PPII.

The peptide Ac-GPPDfpPPGY-NH_2 has the possibility of 32 ($=2^5$) species in slow exchange, due to *cis–trans* isomerism at 5 X–Pro amide bonds. However, this peptide exhibited only one major species by ^{19}F NMR in water, with only very small amounts of species with *cis*-Pro observed, consistent with CD data that PPII was adopted in the model peptide (Figure 9). In contrast, much higher populations of species with *cis*-proline amide bonds were observed both in acetonitrile and in DMSO, which is observable in the large number of minor peaks present in the ^{19}F NMR spectra in these solvents. Interestingly, the major species in both organic solvents also

had a larger difference in ^{19}F chemical shifts of the fluorines, suggesting a stronger preference for one ring pucker in these solvents compared to in water. In contrast, the ^{19}F NMR spectrum in 8 M urea exhibited one major species, with just a single major peak in the ^{19}F NMR spectrum, indicating that similar populations of the *endo* and *exo* ring puckers were present.

These results were confirmed by CD and NMR data on Ac-GPPDfpPPGY-NH_2 as a function of concentration of urea (Figures 9cd). As expected, higher concentrations of urea resulted in higher populations of PPII by CD. However, in contrast to expectations, increased PPII by CD correlated with smaller chemical shift differences between the diastereotopic fluorines. These results indicate that PPII is most favorable when the proline ring adopts *both* ring puckers in similar populations. This result stands in stark contrast to the implications of extensive data with 4-substituted prolines, which has suggested that the *exo* ring pucker (favored by 4*R*-substituted hydroxyprolines and 4*R*-fluoroproline) promotes PPII, while the *endo* ring pucker (favored by 4*S*-substituted hydroxyprolines and 4*S*-fluoroproline) relatively disfavors PPII, compared to proline.[44,86-88] Herein, using Dfp as a probe of proline ring pucker, we identify that the highest population of PPII is present when *both* proline ring puckers are present in similar populations. This result is logical from both entropic and enthalpic perspectives: selection of one ring pucker over the other would be inherently energetically unfavorable. The results herein suggest that urea promotes PPII in part by making the *endo* and *exo* proline ring puckers equienergetic, and thus equally populated, resulting in neither an entropic cost nor an enthalpic cost for adopting PPII. These data are also consistent with urea strongly promoting PPII via solvation of the acceptor carbonyl for $n\rightarrow\pi^*$ interactions, as we recently proposed.[81]

Quantifying proline cis-trans isomerization and identifying induced order in peptides from an intrinsically disordered protein. Finally, we examined the use of Dfp to quantify proline

cis-trans isomerism in model peptides consisting of residues 403-406 from the C-terminal domain of the *tau* protein, whose misfolding and aggregation are associated with neurodegeneration in Alzheimer's disease.[48,52,89-91] We previously observed that both Ser404 phosphorylation and the R406W modification lead to increased population of *cis*-Pro405, both in the shorter $tau_{403–406}$ peptides Ac-TSPR-NH_2 and Ac-TSPW-NH_2 and in larger $tau_{395-411}$ peptides.[54] The data in shorter peptides recapitulated the data in larger *tau* peptides, whose analysis was complicated by the intrinsically disordered nature of these sequences, which results in poor ^{1}H chemical shift dispersion. Using Dfp, we observed similar effects of phosphorylation and the R406W modification on increasing the population of *cis*-proline as was observed by ^{1}H NMR, but with much easier data interpretation due to the simplified nature of ^{19}F NMR spectra (Figure 10, Table 2). In addition, in our prior work we proposed that the combination of *both* Ser-404 phosphorylation *and* the R406W modification (Figure 10c, bottom) would lead to increased order, in both the *trans*-proline and *cis*-proline rotamers, due to the promotion of turn conformations. The ^{19}F NMR data are consistent with increased ordering in *both* proline amide rotamers, based on increased dispersion of the ^{19}F chemical shifts. These results indicate that Dfp can be employed both to quantify proline *cis-trans* isomerization in complex peptides and to identify increased order in peptides, independent of proline amide isomerization state. These results should be broadly applicable to probe protein folding, protein misfolding, and changes in protein structure due to post-translational modifications, protein mutations, and protein-protein interactions.

Discussion

Proline *cis–trans* isomerism is a relatively slow conformational equilibrium (typical half-lives of seconds to minutes) due to the partial double-bond character of the amide bond restricting bond rotation.[1-3,12,55,92] In addition, proline *cis* and *trans* amide bonds are structurally distinct in their relative positioning of the N-terminal and C-terminal protein chains.[2,93,94] Based on these kinetic and structural effects, proline *cis–trans* isomerism can be a rate-determining step in protein folding, and can result in structural and functional switches within proteins.[1,93-95] Despite this fundamental importance of proline conformation on protein structure and dynamics, there is an absence of convenient tools to rapidly interrogate proline *cis–trans* isomerism.

In 2001, Moroder and coworkers demonstrated that 4,4-difluoroproline (Dfp) has potentially unique properties.[17] Dfp is sterically similar to proline, allowing its substitution within proteins and at protein-protein interfaces.[19] Indeed, proline can be replaced by Dfp in expressed proteins using proline-auxotrophic bacteria and incubation with Dfp, as demonstrated both in globular proteins and in elastin.[17,23] Moreover, in contrast to the monosubstituted 4*R*- and 4*S*-fluoroprolines, Dfp has a minimal effect on proline conformational preferences.[13,15,17-19,21] Thus, as either simple acetylated amino acids or within peptides, Dfp and Pro exhibit similar relative populations of *cis* and *trans* amide bonds, as well as similar overall conformational preferences. Consistent with the NMR data on model compounds, both the globular protein barstar and collagen model peptides have similar T_m values in their native forms with proline or with Pro substituted by Dfp.[17,18]

One notable distinction between proline and Dfp is dynamic: Dfp exhibits a modestly (~1 kcal/mol) reduced activation barrier for *cis–trans* isomerism compared to proline.[17] Thus, Dfp could serve to accelerate protein folding or misfolding when proline *cis–trans* isomerism is rate limiting. In a dramatic example, Hilvert and coworkers demonstrated that β2-microglobulin

exhibits dynamic *cis–trans* isomerization at Pro32, with the *cis* conformation favoring the native state, but the *trans* conformation favoring protein misfolding and aggregation.[36] This misfolding is enhanced by low pH, at which histidine is protonated and electronically disfavors an aromatic-proline C–H/π interaction that stabilizes the *cis* conformation.[42,96] Hilvert further demonstrated that replacement of Pro32 with Dfp substantially enhanced β2-microglobulin aggregation and amyloid formation, via the reduced *cis-trans* isomerization activation barrier of Dfp, which allowed the protein to more rapidly sample the aggregation-prone *trans* conformation.

Curiously, neither Moroder nor Conticello reported the ^{19}F NMR spectra of proteins containing Dfp.[17,23] In our work on Dfp within model peptides,[15] we found the ^{19}F NMR spectrum of the peptide Ac-TYDfpN-NH_2 to be similarly curious, with only a singlet observed for the *trans* conformation (Figure 4a), despite two diastereotopic fluorines that should furthermore exhibit strong $^2J_{FF}$ coupling. In the *trans* conformation, the chemical shifts of the diastereotopic fluorines were similar (rendering them magnetically equivalent here), whereas these chemical shifts were highly dispersed in the *cis* amide conformation. Hilvert subsequently made similar observations within β2-microglobulin.[36] These data suggested the possibility that Dfp might be used as a sensitive ^{19}F NMR-based probe of proline *cis-trans* isomerism. In contrast to methods based on differences in ^{13}C chemical shift of proline Cβ and Cγ,[7-10] which require either complete NMR resonance assignment, high peptide or protein concentrations, and/or the use of expensive ^{13}C-labeled proline, Dfp provides a highly practical approach to interrogate proline conformational state. The rapidity of this approach, due to the sensitivity of ^{19}F NMR spectroscopy and the absence of additional resonances in the spectrum, provides an additional advantage in its greater temporal resolution (faster spectral acquisition allowing more frequent analysis of kinetics) compared to ^{13}C NMR-based methods. Due to its commercial availability

(both as Boc-Dfp-OH and Fmoc-Dfp-OH) and its ability to be incorporated in proteins genetically via proline-auxotrophic bacteria,[17,23] Dfp might represent a unique tool for the rapid determination of the *cis-trans* isomerization state of prolines, within proteins and for the investigation of mechanisms of protein folding and assembly.

Dfp can be site-specifically incorporated at the site of a single proline, via standard solid-phase peptide synthesis in peptides, or via the combination of synthetic peptides and/or expressed proteins using native chemical ligation and/or expressed proteins using expressed protein ligation/protein semisynthesis.[97,98] Using these technologies, Dfp can be employed to rapidly and exquisitely probe protein conformation at proline, via simple 1–D ^{19}F NMR spectroscopy, with the absence of complications from other residues, from H_2O, or from other small molecules in solution. Indeed, ^{19}F NMR is extensively used to understand protein folding and other biological processes in complex media, including whole cells.[28-30,99-101] Herein, Dfp was applied both to quantify proline *cis-trans* isomerism, and to identify order versus disorder, via the difference in the chemical shifts of the diastereotopic fluorines. The observation of similar ^{19}F chemical shifts of the fluorines indicates inherent disorder, that is, structures in which both the *endo* and *exo* proline ring puckers are present in similar populations. In contrast, the observation of distinct chemical shifts of the diastereotopic fluorines is associated with local or global order, as it indicates a significant preference for one proline ring pucker over the other. Intrinsically disordered proteins (IDPs) are critical in cellular function, and changes in protein structure, including proline *cis-trans* isomerism, in IDPs have been implicated in disease.[102-104] More broadly, proline is specially situated as a locus for order and for intermolecular interactions, both within IDPs and within globular proteins.[92,94,105,106] However, identification of these structural changes, especially at proline, poses significant challenges.[107,108] The results herein suggest that

Dfp might be uniquely useful for the practical identification of order, disorder, and proline *cis-trans* isomerism in proteins.

Experimental

Small molecule synthesis. **3**, **6**, and **7** were synthesized from commercially available **1** using variations on previously described approaches.[16-18] Synthesis, purification, and characterization details are in the Supporting Information.

X-ray crystallography. **3** crystallized via slow evaporation of a solution of **3** in $CDCl_3$. Details of crystal structure determination are in the Supporting Information. The crystallographic information files of **3** have been deposited with the Cambridge Crystallographic Data Centre under CCDC 1566681 (data collection at 200 K) and CCDC 2279640 (data collection at 100 K).

Peptide synthesis. Peptides were synthesized by standard Fmoc solid-phase peptide synthesis and purified to homogeneity. Synthesis, purification, and conformational analysis of the peptide Ac-TYDfpN-NH_2 were described previously.[13,15] Synthesis, purification, and characterization details of other peptides are in the Supporting Information.

^{19}F NMR spectroscopy. Solution-state ^{19}F NMR spectroscopy was conducted on a Brüker 400 MHz NMR spectrometer with a BBFO probe or with a cryogenic QNP probe. Resonances were referenced internally to residual TFA (δ = –76.55 ppm). Solid-state magic-angle spinning ^{19}F NMR spectroscopy was conducted on a Brüker AVIII 500 MHz NMR spectrometer with a 4 mm Brüker HX probe, using spinning rates of 13 kHz and 15 kHz. Solid-state ^{19}F NMR spectra were referenced externally with 5-F-tryptophan. Additional data and

analysis, including ^{1}H NMR data on compounds, expanded views of ^{19}F NMR spectra, and compilations of spectral data, are in the Supporting Information.

Circular dichroism. CD spectra were recorded on a Jasco J-810 or a Jasco J-1500 spectropolarimeter. Data represent the average of at least three independent trials. Data were averaged but were not smoothed.

Computational chemistry. Calculations were conducted with Gaussian 09.[109] Geometry-optimized structures of Ac-Dfp-OMe, Piv-Dfp-OMe, Ac-Dfp-NMe_2, and Piv-Dfp-NMe_2 were generated, with variation of main-chain conformation (α versus PPII), ring pucker (*exo* versus *endo*), proline amide rotamer (*ω* torsion angle, *trans* versus *cis*), and implicit solvent (H_2O versus $CHCl_3$). Final geometry optimization calculations were conducted using the M06-2X DFT functional and the 6-311++G(3d,3p) basis set with IEFPCM implicit solvation.[110-112] NMR shielding parameters were then calculated using the GIAO method and the same combinations of functional, basis set, and solvation model.[113,114] ^{19}F chemical shifts in Dfp were referenced to those of TFA, based on the average calculated chemical shifts of the fluorines in TFA, which had been geometry optimized using the same methods as molecules with Dfp. Calculations on **3**•$CHCl_3$ were conducted using the coordinates from the crystal structure file, with the positions of the heavy atoms fixed (optimization of H atoms only) based on those observed crystallographically, or alternatively with the positions of the heavy atoms other than fluorine fixed (optimization of H and F atoms). The minimal version of **3** (EtOCO-Dfp-OH) was generated via computational removal of the Fmoc aromatic carbon atoms and the addition of hydrogen atoms on the missing valences in the resulting ethyl group within GaussView, followed by restrained geometry optimization and calculation of the NMR shielding parameters. Additional details of calculations are in the Supporting Information.

Acknowledgements

We thank NSF (CHE-1412978, CHE-2004110, BIO-1616490) and the DOD PRARP program (AZ140115) for funding. Instrumentation support was provided by NIH (GM110758) and NSF (CHE-1229234).

Supporting Information Available

^{1}H, ^{13}C, and ^{19}F NMR spectra for synthesized small molecules, CD spectra, and full synthesis and characterization data of all peptides, as well as additional ^{19}F NMR data. This material is available free of charge via the Internet at the journal web site.

Figures

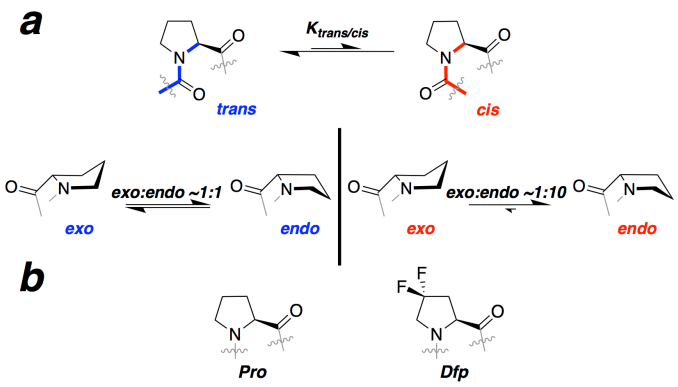

Figure 1. (a) Summary of conformational equilibria and preferences of the proline (top) amide bond and (bottom) ring pucker. (b) Comparison of proline with 4,4-difluoroproline (Dfp).

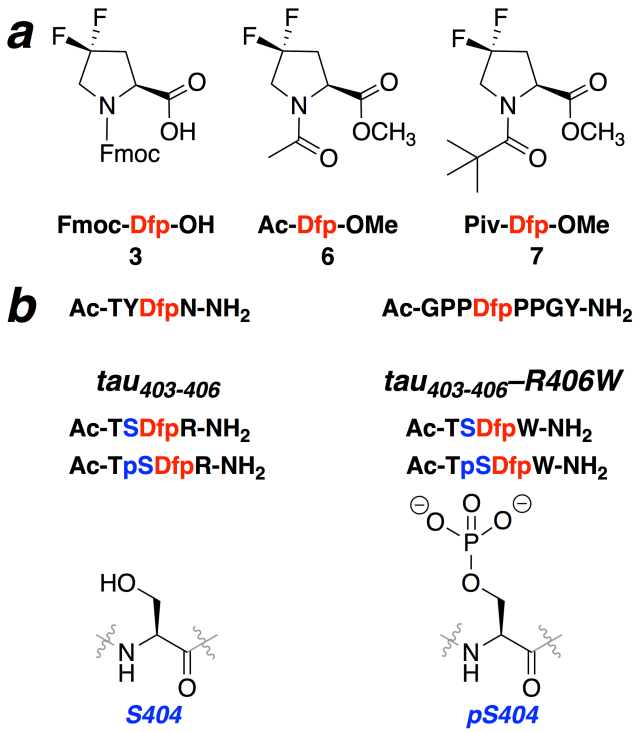

Figure 2. Summary of compounds and peptides examined herein. (a) Acyl capping groups were installed on Dfp to generate Ac-Dfp-OMe (**6**) and Piv-Dfp-OMe (**7**). The pivaloyl group strongly promotes intercarbonyl $n\rightarrow\pi^*$ interactions and the *trans*-proline amide rotamer. Synthesis and characterization of **6** and **7** are described in the Supporting Information. (b) Dfp was incorporated into model peptides and into tetrapeptides derived from the *tau* C-terminal domain.

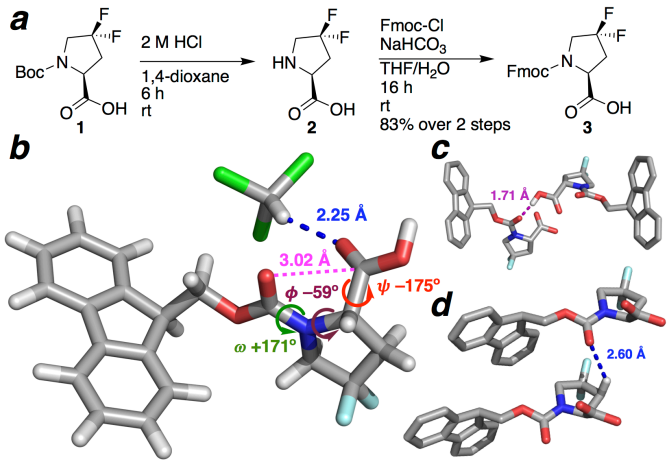

Figure 3. (a) Synthesis of Fmoc-Dfp-OH (**3**) from commercially available Boc-Dfp-OH (**1**). (b) Crystal structure (100 K data collection) of Fmoc-Dfp-OH•$CHCl_3$. The structure exhibited a close C–H/O interaction (blue) between the carboxylic acid carbonyl and the C–H of chloroform. (c) Crystal assembly of Fmoc-Dfp-OH is mediated in part via hydrogen bonding between the carboxylic acid hydrogen and the carbamate carbonyl of an adjacent molecule. (d) Intermolecular C–H/O interaction between Pro C–Hβ and an adjacent carbonyl. Bond lengths to hydrogen were normalized in Mercury.

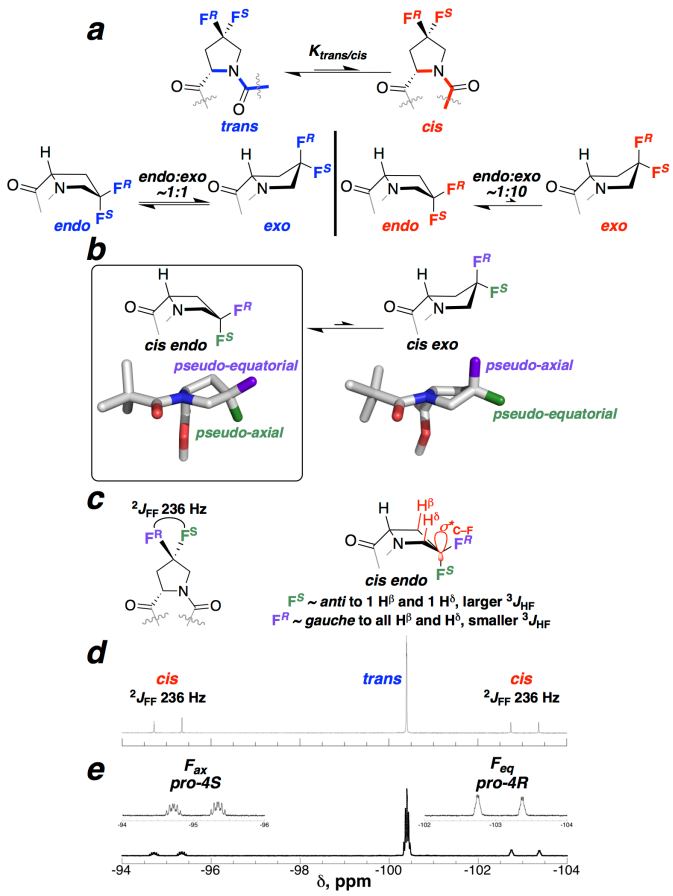

Figure 4. (a) Summary of the conformational equilibria and preferences of the Dfp amide bond and ring pucker. (b) The *pro*-4*S* fluorine is pseudo-axial in an *endo* ring pucker and pseudo-equatorial in an *exo* ring pucker, while the opposite is observed for the *pro*-4*R* fluorine. The structures shown are for a model with *cis*-proline, but similar relationships of the diastereotopic fluorines are present for *trans*-proline. Pseudo-axial fluorines are approximately *anti*-periplanar to 1 Hβ and 1 Hγ and thus exhibit larger $^{3}J_{HF}$ coupling constants with these hydrogens, while pseudo-equatorial fluorines are *gauche* to both Hβ and to both Hδ hydrogens, and thus exhibit only smaller coupling constants with these hydrogens. (c) The diastereotopic fluorines exhibit strong $^{2}J_{FF}$ coupling, which causes each fluorine resonance to appear a doublet, as is observed here in the *cis* conformation. The larger $^{3}J_{HF}$ observed for the pseudo-axial fluorine are due to orbital overlap between σ^*_{C-F} and the σ_{C-H}, which also leads to longer C–F bonds for the pseudo-axial fluorines. (d) ^{1}H-decoupled and (e) ^{1}H-coupled ^{19}F NMR spectra of the peptide Ac-TYDfpN-NH_2 in 90% H_2O/10% D_2O with 5 mM phosphate buffer pH 4.0 and 25 mM NaCl. The *cis* peaks are shown in the inset, expanded to emphasize the differences in ^{1}H-^{19}F coupling in the predominantly pseudo-axial fluorine (downfield) versus the predominantly pseudo-equatorial fluorine (upfield).

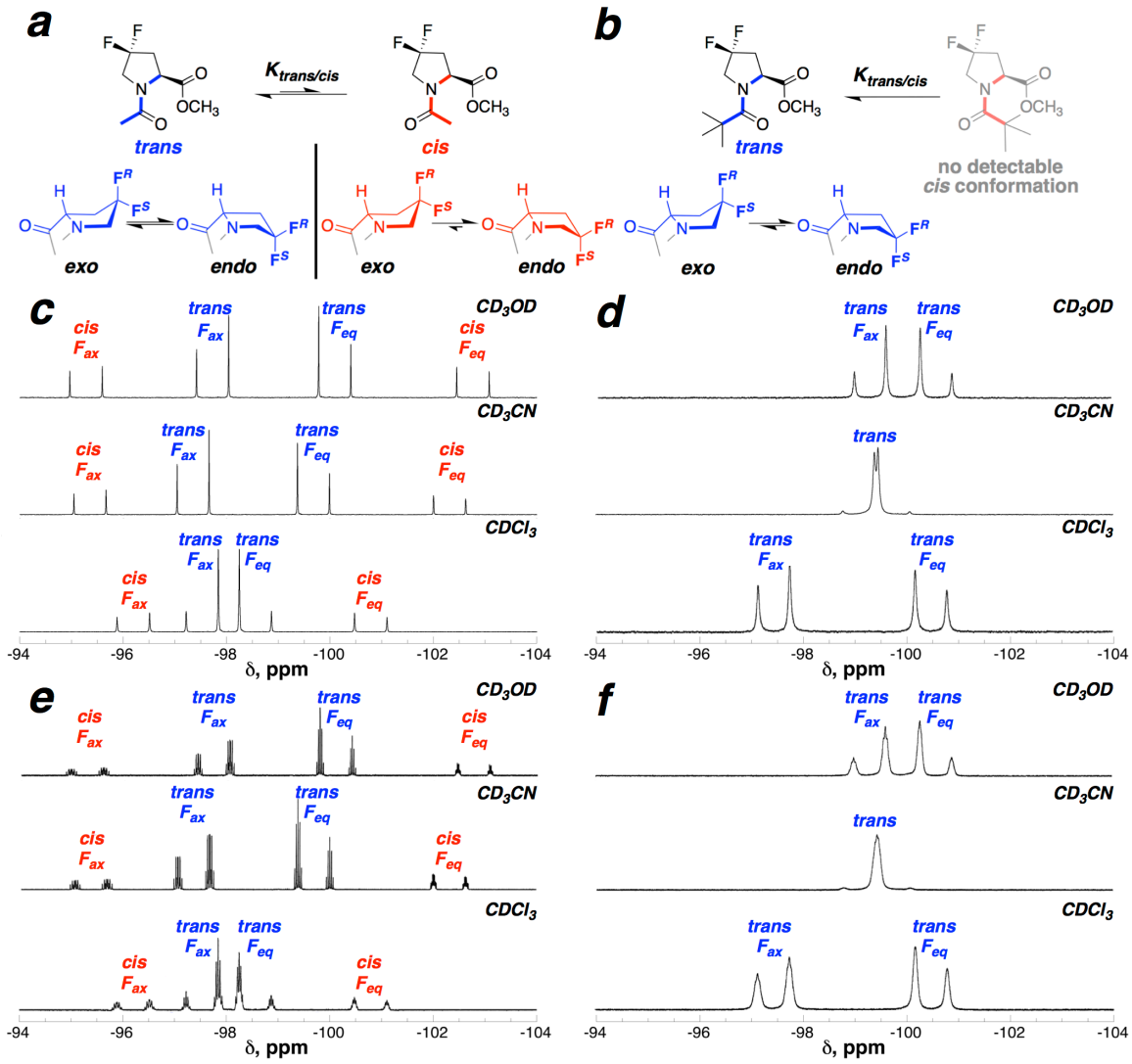

Figure 5. Solvent-dependent ^{19}F NMR spectra of (left) Ac-Dfp-OMe and (right) Piv-Dfp-OMe. (a) Ac-Dfp-OMe conformational equilibria: *cis-trans* amide isomerization and ring pucker interconversion. (b) Piv-Dfp-OMe conformational equilibria: only the *trans* amide conformation was observed. (c,d) Solvent dependent ^{1}H-decoupled ^{19}F NMR spectra of (c) Ac-Dfp-OMe and (d) Piv-Dfp-OMe, (e,f) Solvent-dependent ^{1}H-coupled ^{19}F NMR spectra of (e) Ac-Dfp-OMe and (f) Piv-Dfp-OMe. Data were collected at 298 K. For spectra with Piv-Dfp-OMe, broadening is observed due to proline *cis-trans* isomerization that is in intermediate exchange on the NMR timescale at this temperature. The assignment of the *endo* ring pucker as the main ring pucker for Ac-*cis*-Dfp-OMe is further supported by the Hα resonances of the ^{1}H NMR spectra, which exhibit simplified coupling patters compared to the Hα resonances for *trans*-Dfp, with the *cis*-Dfp coupling pattern consistent with that expected for an *endo* ring pucker as the dominant species; see the Supporting Information for details. F_{ax} indicates the diastereotopic fluorine which is pseudo-axial in the major proline ring pucker, while F_{eq} indicates the diastereotopic fluorine which is pseudo-equatorial in the major proline ring pucker in the indicated proline amide conformation under the described conditions.

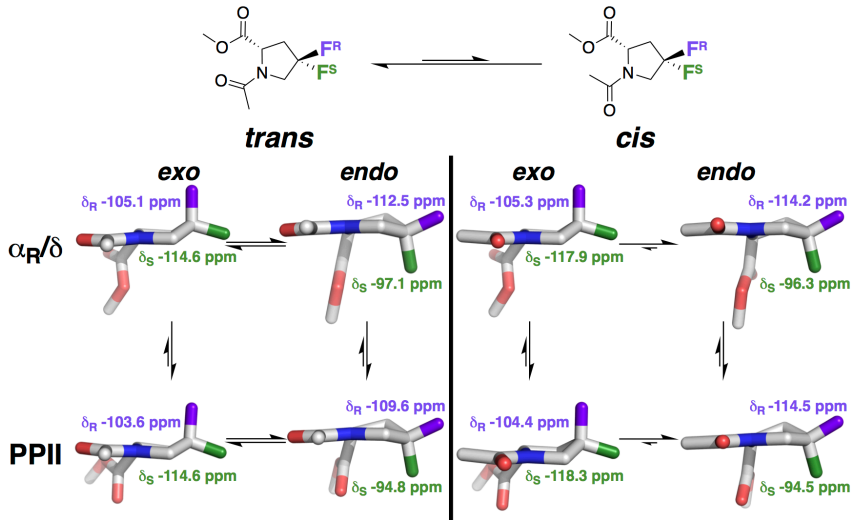

Figure 6. Geometry-optimized structures of Ac-Dfp-OMe in implicit water in the *trans* and *cis* amide conformations, each with the *exo* and *endo* ring puckers in the indicated regions of Ramachandran space. The calculated ^{19}F chemical shifts for the *pro*-4*R* (purple) and *pro*-4*S* (green) fluorines are indicated in each conformation. Equivalent ^{19}F NMR analysis for Piv-Dfp-OMe, Ac-Dfp-NMe$_2$, and Piv-Dfp-NMe$_2$ as a function of conformation are in the Supporting Information. ^{19}F NMR chemical shifts were calculated using the GIAO method with the M06-2X functional and the 6-311++G(3d,3p) basis set in implicit water. Additional details on the conformations, including their relative energies, as well as coordinates for all structures in implicit H_2O and implicit $CHCl_3$ are in the Supporting Information.

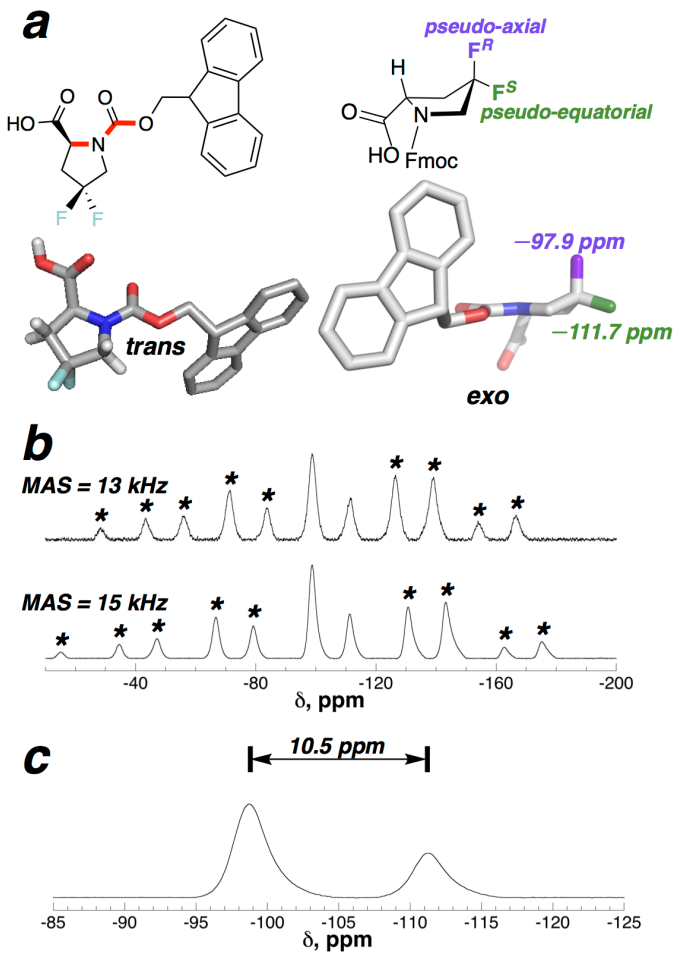

Figure 7. Solid-state ^{19}F NMR spectroscopy of Fmoc-Dfp-OH in the crystalline form. (a) Crystal structure of Fmoc-Dfp-OH in the *trans*-proline conformation, which exhibits an *exo* ring pucker, with the *pro*-4*R* (purple) and *pro*-4*S* (green) fluorines indicated. (b) Solid-state ^{19}F NMR spectra of crystalline Fmoc-Dfp-OH. The spectra were obtained using magic-angle spinning (MAS) with spinning frequencies of 13 kHz and 15 kHz. The central bands of the spectra, with chemical shifts of –98.7 ppm and –111.2 ppm, correspond to the *pro*-4*R* and *pro*-4*S* fluorines, respectively. All other signals present in the spectra are spinning side bands (indicated with asterisks). The spectra were referenced with external polycrystalline 5F-Trp at 87.0 ppm, as a secondary reference to CCl_3F at 0 ppm. (c) Expanded view of the central bands in the MAS ^{19}F NMR spectra of crystalline Fmoc-Dfp-OH, revealing a chemical shift difference (Δδ) of 10.5 ppm between the fluorines assigned as the *pro*-4*R* (downfield) and *pro*-4*S* (upfield) fluorines. Additional details are in the Supporting Information.

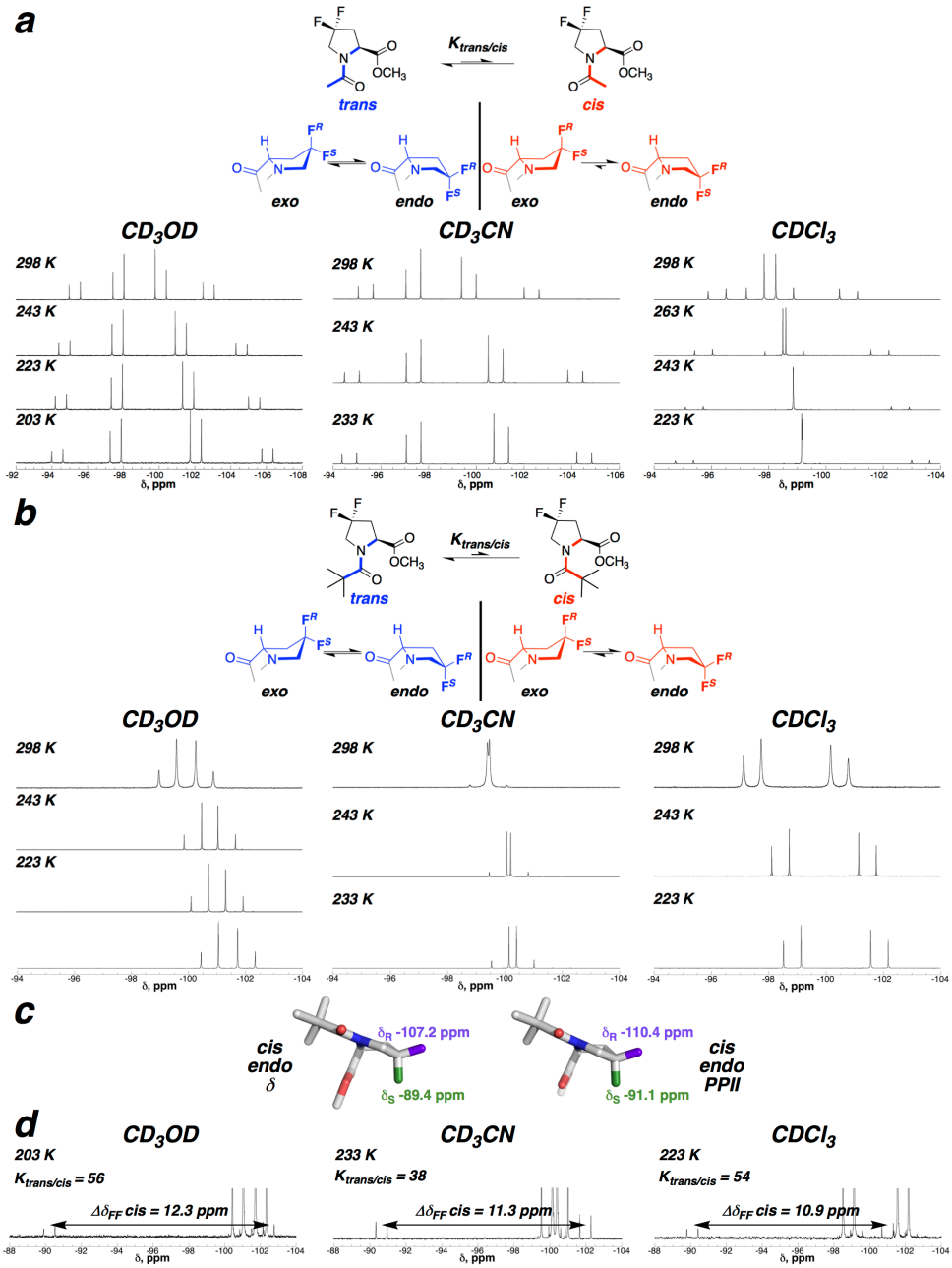

Figure 8. Temperature-dependent ^{1}H-decoupled ^{19}F NMR spectra of (a) Ac-Dfp-OMe and (b) Piv-Dfp-OMe in CD_3OD, CD_3CN, and $CDCl_3$. (c) Calculated optimized structures and ^{19}F chemical shifts of Piv-Dfp-OMe in $CHCl_3$ with *cis*-proline and an *endo* ring pucker. Calculations indicated a ≥ 2 kcal mol^{-1} preference for the *endo* versus the *exo* ring pucker in Piv-*cis*-Dfp-OMe. Structures were subjected to NMR calculations using the GIAO method with the M06-2X functional and the 6-311++G(3d,3p) basis set. (d) Low-temperature ^{19}F NMR spectra of Piv-Dfp-OMe, with expansion of the chemical shift range and truncation of the *trans*-proline peaks in order to emphasize the minor *cis*-proline peaks, in CD_3OD, CD_3CN, and $CDCl_3$. The peak broadening observed for Piv-Dfp-OMe at 298 K is likely due to its lower barrier for the *cis*-to-*trans* isomerization compared to Ac-Dfp-OMe, which causes its spectrum to represent intermediate exchange (broadening) rather than slow exchange on the NMR timescale.

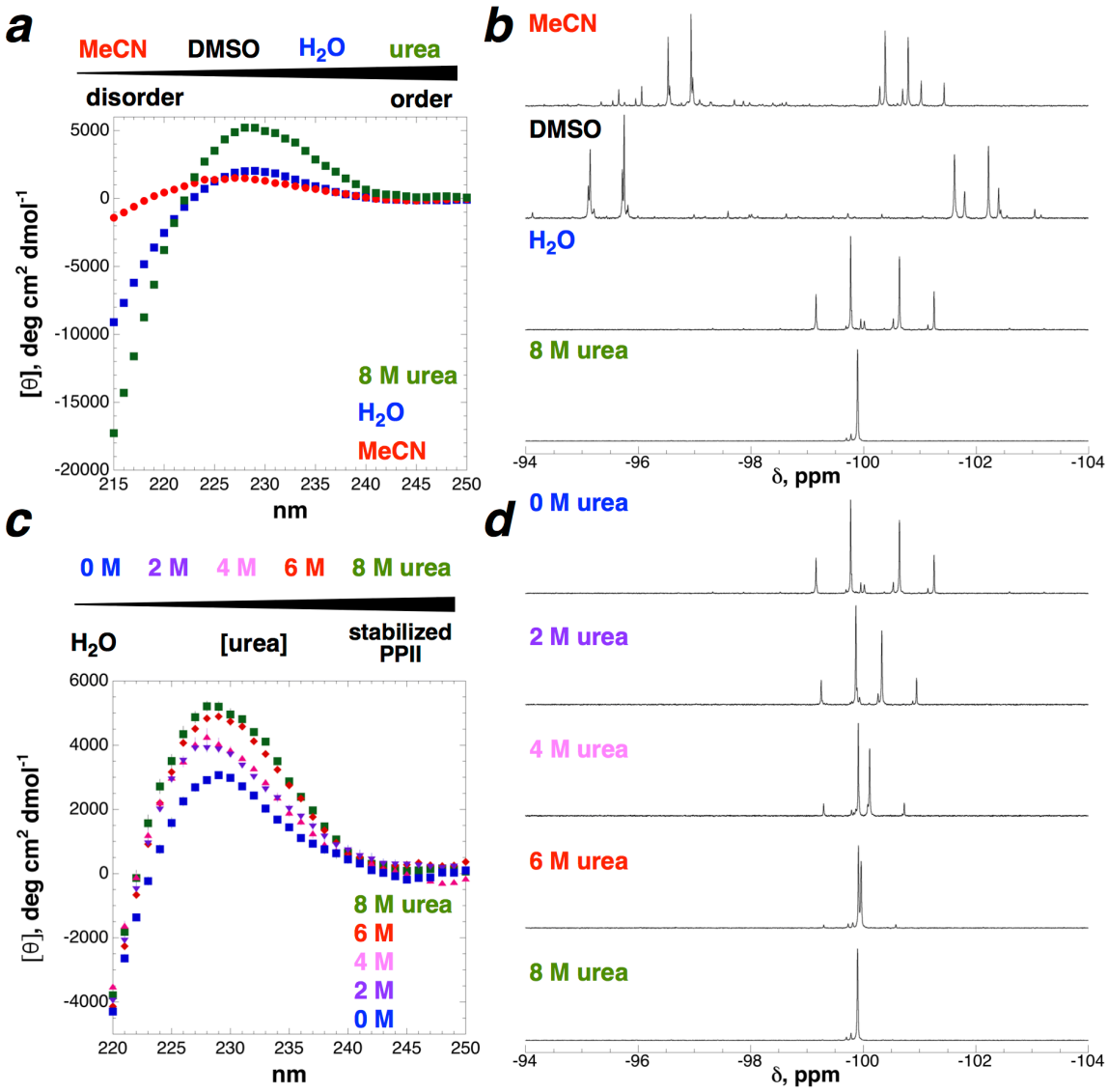

Figure 9. ^{19}F NMR and circular dichroism (CD) spectroscopy of the model peptide Ac-GPPDfpPPGY-NH_2 as a function of solvation. (a) CD spectra in buffered H_2O (with 5 mM phosphate pH 4 and 25 mM KF), acetonitrile, and 8 M urea. Experiments were conducted at 25 °C. Data represent the average of at least three independent trials. (b) ^{1}H-decoupled ^{19}F NMR spectra as a function of solvent. (c) CD spectra as a function of urea concentration. (d) ^{1}H-decoupled ^{19}F NMR spectra as a function of urea concentration. Experiments in organic solvents and experiments in (c) and (d) were conducted without added buffer or salt. ^{1}H NMR spectra of the peptide in buffered H_2O, in DMSO, and in acetonitrile, as well as temperature-dependent ^{1}H and ^{19}F NMR spectra in buffered H_2O, are in Supporting Information.

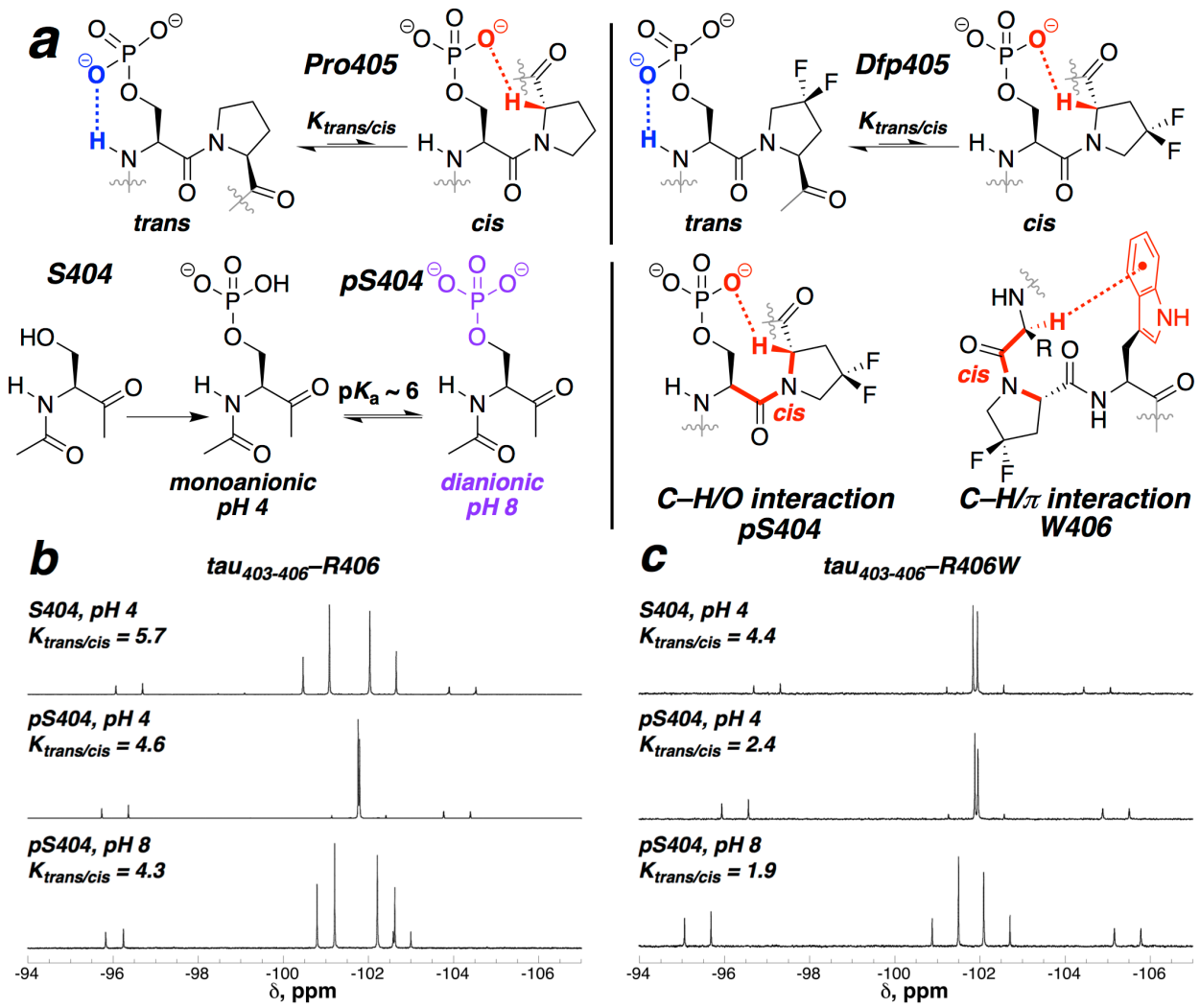

Figure 10. (a) Phosphorylation of serine stabilizes the *trans*-proline and *cis*-proline conformations via an intraresidue phosphate-amide hydrogen bond and a phosphate-ProHα C-H/O interaction, respectively. This effect is dependent on the ionization state of the phosphate, with the strongest effects observed in the dianionic form of phosphoserine. The R406W modification induces C–H/π interactions which further stabilize the *cis*-proline conformation, but also promote turn conformations in *trans*-proline. (b) ^{1}H-decoupled ^{19}F NMR spectra of $tau_{403-406}$ R406 peptides as a function of phosphorylation and ionization state of the phosphate. The phosphorylated peptide has an increased *cis* population relative to the non-phosphorylated peptide at pH 4.0, and this population increases when the phosphate is dianionic. (c) ^{1}H-decoupled ^{19}F NMR spectra of $tau_{403-406}$ R406W peptides as a function of phosphorylation and ionization state of the phosphate. The non-phosphorylated R406W peptide has an increased *cis*-proline population in comparison to the native R406 peptide, and this effect further increases upon phosphorylation. ^{1}H-coupled ^{19}F NMR spectra, ^{1}H NMR spectra, TOCSY spectra, and summaries of the NMR data for each peptide are in the Supporting Information.

Tables

Table 1. Summary of temperature-dependent ^{19}F NMR data for Ac-Dfp-OMe and Piv-Dfp-OMe as a function of solvent.

	Solvent	Temperature, K	$K_{trans/cis}$	*cis* downfield δ, ppm	*cis* upfield δ, ppm	*cis* $\Delta\delta_{FF}$, ppm	*trans* downfield δ, ppm	*trans* upfield δ, ppm	*trans* $\Delta\delta_{FF}$, ppm
Ac-Dfp-OMe	CD_3OD	298	2.4	–95.3	–102.8	7.5	–97.7	–100.1	2.4
		243	2.6	–94.7	–104.6	9.9	–97.7	–101.2	3.5
		223	2.6	–94.5	–105.3	10.8	–97.6	–101.6	4.0
		203	2.5	–94.3	–106.1	11.8	–97.6	–102.1	4.5
	CD_3CN	298	2.3	–95.4	–102.3	6.9	–97.4	–99.7	2.3
		243	2.7	–94.8	–104.1	9.3	–97.4	–100.8	3.4
		233	2.8	–94.7	–104.5	9.8	–97.4	–101.0	3.6
	$CDCl_3$	298	3.1	–96.2	–100.8	4.6	–97.5	–98.6	1.1
		263	3.7	–95.7	–101.9	6.2	–98.2	–98.9	0.7
		243	4.0	–95.4	–102.6	7.2	–98.5	–99.2	0.7
		223	4.1	–95.1	–103.3	8.2	–98.8	–99.5	0.7
Piv-Dfp-OMe	CD_3OD	298	n.d.	—	—	—	–99.3	–100.6	1.3
		243	30	–91.0	–101.6	10.6	–100.2	–101.2	1.0
		223	37	–90.6	–102.0	11.4	–100.5	–101.8	1.3
		203	56	–90.2	–102.5	12.3	–100.8	–102.0	1.2
	CD_3CN	298	n.d.	—	—	—	–99.1	–99.8	0.7
		243	32	–90.9	–101.7	10.8	–99.8	–100.5	0.7
		233	38	–90.7	–102.0	11.3	–99.8	–100.7	0.9
	$CDCl_3$	298	n.d.	—	—	—	–97.4	–100.5	3.1
		243	37	–90.6	–100.5	9.9	–98.4	–101.5	3.1
		223	54	–90.1	–101.0	10.9	–98.8	–101.9	3.1

Table 2. Summary of ^{19}F NMR data of $tau_{403\text{-}406}$ peptides as a function of phosphorylation, residue 406 identity, and pH.

peptide	pH	$K_{trans/cis}$	*cis* $\delta_{downfield}$, ppm	*cis* $\delta_{upfield}$, ppm	*cis* $\Delta\delta_{FF}$, ppm	*trans* $\delta_{downfield}$, ppm	*trans* $\delta_{upfield}$, ppm	*trans* $\Delta\delta_{FF}$, ppm
TSDfpR	4.0	5.7	–96.3	–104.2	7.9	–100.8	–102.3	1.5
TpSDfpR	4.0	4.6	–96.1	–104.0	7.9	–101.4	–102.1	0.7
	6.5	3.9	–96.1	–102.9	6.8	–101.1	–102.3	1.2
	7.2	4.1	–96.0	–102.8	6.8	–101.0	–102.4	1.4
	8.0	4.3	–96.0	–102.8	6.8	–101.0	–102.4	1.4
TSDfpW	4.0	4.4	–97.0	–104.8	7.8	–101.5	–102.3	0.8
TpSDfpW	4.0	2.4	–96.3	–105.2	8.9	–101.6	–102.3	0.7
	6.5	1.9	–95.6	–105.4	9.8	–101.3	–102.4	1.1
	7.2	2.0	–95.4	–105.5	10.1	–101.2	–102.4	1.2
	8.0	1.9	–95.4	–105.5	10.1	–101.2	–102.4	1.2

References

(1) Brandts, J. F.; Halvorson, H. R.; Brennan, M. Consideration of the possibility that the slow step in protein denaturation reactions is due to cis-trans isomerization of proline residues. *Biochemistry* **1975**, *14*, 4953-4963.

(2) Fischer, G. Chemical aspects of peptide bond isomerisation. *Chem. Soc. Rev.* **2000**, *29*, 119-127.

(3) Eckert, B.; Martin, A.; Balbach, J.; Schmid, F. X. Prolyl isomerization as a moleular timer in phage infection. *Nature Struct. Mol. Biol.* **2005**, *12*, 619-623.

(4) Lippens, G.; Landrieu, I.; Smet, C. Molecular mechanisms of the phospho-dependent prolyl cis/trans isomerase Pin1. *FEBS J.* **2007**, *274*, 5211-5222.

(5) Lu, K. P.; Finn, G.; Lee, T. H.; Nicholson, L. K. Prolyl cis-trans isomerization as a molecular timer. *Nat. Chem. Biol.* **2007**, *3*, 619-629.

(6) Mallis, R. J.; Brazin, K. N.; Fulton, D. B.; Andreotti, A. H. Structural characterization of a proline-driven conformational switch within the Itk SH2 domain. *Nature Struct. Biol.* **2002**, *9*, 900-905.

(7) Deber, C. M.; Bovey, F. A.; Carver, J. P.; Blout, E. R. Nuclear Magnetic Resonance Evidence for Cis-Peptide Bonds in Proline Oligomers. *J. Am. Chem. Soc.* **1970**, *92*, 6191-6198.

(8) Dorman, D. E.; Bovey, F. A. C-13 Magnetic-Resonance Spectroscopy - Spectrum of Proline in Oligopeptides. *J. Org. Chem.* **1973**, *38*, 2379-2383.

(9) Dorman, D. E.; Torchia, D. A.; Bovey, F. A. C-13 and Proton Nuclear Magnetic-Resonance Observations of Conformation of Poly(L-Proline) in Aqueous Salt Solutions. *Macromolecules* **1973**, *6*, 80-82.

(10) Siemion, I. Z.; Wieland, T.; Pook, K. H. Influence of Distance of Proline Carbonyl from Beta and Gamma Carbon on C-13 Chemical-Shifts. *Angew. Chem., Int. Ed.* **1975**, *14*, 702-703.

(11) Stewart, D. E.; Sarkar, A.; Wampler, J. E. Occurrence and role of cis peptide-bonds in protein structures. *J. Mol. Biol.* **1990**, *214*, 253-260.

(12) Pal, D.; Chakrabarti, P. Cis Peptide Bonds in Proteins: Residues Involved, their Conformations, Interactions and Locations. *J. Mol. Biol.* **1999**, *294*, 271-288.

(13) Thomas, K. M.; Naduthambi, D.; Tririya, G.; Zondlo, N. J. Proline Editing: A Divergent Strategy for the Synthesis of Conformationally Diverse Peptides. *Org. Lett.* **2005**, *7*, 2397-2400.

(14) Naduthambi, D.; Zondlo, N. J. Stereoelectronic tuning of the structure and stability of the trp cage miniprotein. *J. Am. Chem. Soc.* **2006**, *128*, 12430-12431.

(15) Pandey, A. K.; Naduthambi, D.; Thomas, K. M.; Zondlo, N. J. Proline Editing: A General and Practical Approach to the Synthesis of Functionally and Structurally Diverse Peptides. Analysis of Steric versus Stereoelectronic Effects of 4-Substituted Prolines on Conformation within Peptides. *J. Am. Chem. Soc.* **2013**, *135*, 4333-4363.

(16) Demange, L.; Ménez, A.; Dugave, C. Practical synthesis of Boc and Fmoc Protected 4-Fluoro and 4-Difluoroprolines from Trans-4-Hydroxyproline. *Tetrahedron Lett.* **1998**, *39*, 1169-1172.

(17) Renner, C.; Alefelder, S.; Bae, J. H.; Budisa, N.; Huber, R.; Moroder, L. Fluoroprolines as Tools for Protein Design and Engineering. *Angew. Chem., Int. Ed.* **2001**, *40*, 923-925.

(18) Shoulders, M. D.; Kamer, K. J.; Raines, R. T. Origin of the stability conferred upon collagen by fluorination. *Bioorg. Med. Chem. Lett.* **2009**, *19*, 3859-3862.

(19) Somovilla, V. J.; Bermejo, I. A.; Albuquerque, I. S.; Martinez-Saez, N.; Castro-Lopez, J.; Garcia-Martin, F.; Companon, I.; Hinou, H.; Nishimura, S. I.; Jimenez-Barbero, J.; Asensio, J. L.; Avenoza, A.; Busto, J. H.; Hurtado-Guerrero, R.; Peregrina, J. M.; Bernardes, G. J. L.; Corzana, F. The Use of Fluoroproline in MUC1 Antigen Enables Efficient Detection of Antibodies in Patients with Prostate Cancer. *J. Am. Chem. Soc.* **2017**, *139*, 18255-18261.

(20) Kubyshkin, V.; Davis, R.; Budisa, N. Biochemistry of fluoroprolines: the prospect of making fluorine a bioelement. *Beilstein J. Org. Chem.* **2021**, *17*, 439-460.

(21) Hofman, G. J.; Ottoy, E.; Light, M. E.; Kieffer, B.; Kuprov, I.; Martins, J. C.; Sinnaeve, D.; Linclau, B. Minimising conformational bias in fluoroprolines through vicinal difluorination. *Chem. Commun.* **2018**, *54*, 5118-5121.

(22) Hofman, G. J.; Ottoy, E.; Light, M. E.; Kieffer, B.; Martins, J. C.; Kuprov, I.; Sinnaeve, D.; Linclau, B. Synthesis and Conformational Properties of 3,4-Difluoro-L-prolines. *J. Org. Chem.* **2019**, *84*, 3100-3120.

(23) Kim, W. Y.; George, A.; Evans, M.; Conticello, V. P. Cotranslational incorporation of a structurally diverse series of proline analogues in an Escherichia coli expression system. *ChemBioChem* **2004**, *5*, 928-936.

(24) Lieblich, S. A.; Fang, K. Y.; Cahn, J. K. B.; Rawson, J.; LeBon, J.; Ku, H. T.; Tirrell, D. A. 4S-Hydroxylation of Insulin at ProB28 Accelerates Hexamer Dissociation and Delays Fibrillation. *J. Am. Chem. Soc.* **2017**, *139*, 8384-8387.

(25) Breunig, S. L.; Tirrell, D. A. Incorporation of proline analogs into recombinant proteins expressed in Escherichia coli. *Meth. Enzymol.* **2021**, *656*, 545-571.

(26) O' Loughlin, J.; Napolitano, S.; Rubini, M. Protein Design with Fluoroprolines: 4,4-Difluoroproline Does Not Eliminate the Rate-Limiting Step of Thioredoxin Folding. *ChemBioChem* **2021**, *22*, 3326-3332.

(27) Jäckel, C.; Koksch, B. Fluorine in peptide design and protein engineering. *Eur. J. Org. Chem* **2005**, 4483-4503.

(28) Ruiz-Cabello, J.; Barnett, B. P.; Bottomley, P. A.; Bulte, J. W. M. Fluorine ((19)F) MRS and MRI in biomedicine. *NMR Biomed.* **2011**, *24*, 114-129.

(29) Arntson, K. E.; Pomerantz, W. C. K. Protein-Observed Fluorine NMR: A Bioorthogonal Approach for Small Molecule Discovery. *J. Med. Chem.* **2016**, *59*, 5158-5171.

(30) Salwiczek, M.; Nyakatura, E. K.; Gerling, U. I. M.; Ye, S. J.; Koksch, B. Fluorinated amino acids: compatibility with native protein structures and effects on protein-protein interactions. *Chem. Soc. Rev.* **2012**, *41*, 2135-2171.

(31) Marsh, E. N. G.; Suzuki, Y. Using 19F NMR to Probe Biological Interactions of Proteins and Peptides. *ACS Chem. Biol.* **2014**, *9*, 1242-1250.

(32) Verhoork, S. J. M.; Killoran, P. M.; Coxon, C. R. Fluorinated Prolines as Conformational Tools and Reporters for Peptide and Protein Chemistry. *Biochemistry* **2018**, *57*, 6132-6143.

(33) Killoran, P. M.; Hanson, G. S. M.; Verhoork, S. J. M.; Smith, M.; Del Gobbo, D.; Lian, L.-Y.; Coxon, C. R. Probing Peptidylprolyl Bond cis/trans Status Using Distal 19F NMR Reporters *Chem. Eur. J.* **2023**, *29*, e202203017.

(34) Di Pietrantonio, C.; Pandey, A.; Gould, J.; Hasabnis, A.; Prosser, R. S. Understanding Protein Function Through an Ensemble Description: Characterization of Functional States by 19F NMR. *Meth. Enzymol.* **2019**, *615*, 103-130.

(35) Gimenez, D.; Phelan, A.; Murphy, C. D.; Cobb, S. L. F-19 NMR as a tool in chemical biology. *Beilstein J. Org. Chem.* **2021**, *17*, 293-318.

(36) Torbeev, V. Y.; Hilvert, D. Both the cis-trans equilibrium and isomerization dynamics of a single proline amide modulate beta 2-microglobulin amyloid assembly. *Proc. Natl. Acad. Sci. U.S.A.* **2013**, *110*, 20051-20056.

(37) Costantini, N. V.; Ganguly, H. K.; Martin, M. I.; Wenzell, N. A.; Yap, G. P. A.; Zondlo, N. J. The distinct conformational landscapes of 4S-substituted prolines that promote an endo ring pucker. *Chem. Eur. J.* **2019**, *25*, 11356-11364.

(38) Wenzell, N. A.; Ganguly, H. K.; Pandey, A. K.; Bhatt, M. R.; Yap, G. P. A.; Zondlo, N. J. Electronic and steric control of n→π* interactions via N-capping: stabilization of the α-helix conformation without a hydrogen bond. *ChemBioChem* **2019**, *20*, 963-967.

(39) Meng, H. Y.; Thomas, K. M.; Lee, A. E.; Zondlo, N. J. Effects of *i* and *i*+3 Residue Identity on Cis-Trans Isomerism of the Aromatic$_{i+1}$-Prolyl$_{i+2}$ Amide Bond: Implications for Type VI b-turn Formation. *Biopolymers (Peptide Sci.)* **2006**, *84*, 192-204.

(40) Thomas, K. M.; Naduthambi, D.; Zondlo, N. J. Electronic control of amide cis-trans isomerism via the aromatic-prolyl interaction. *J. Am. Chem. Soc.* **2006**, *128*, 2216-2217.

(41) Brown, A. M.; Zondlo, N. J. A Propensity Scale for Type II Polyproline Helices (PPII): Aromatic Amino Acids in Proline-Rich Sequences Strongly Disfavor PPII Due to Proline-Aromatic Interactions. *Biochemistry* **2012**, *51*, 5041-5051.

(42) Pandey, A. K.; Thomas, K. M.; Forbes, C. R.; Zondlo, N. J. Tunable Control of Polyproline Helix (PPII) Structure via Aromatic Electronic Effects: An Electronic Switch of Polyproline Helix. *Biochemistry* **2014**, *53*, 5307-5314.

(43) Brister, M. A.; Pandey, A. K.; Bielska, A. A.; Zondlo, N. J. OGlcNAcylation and Phosphorylation Have Opposing Structural Effects in tau: Phosphothreonine Induces Particular Conformational Order. *J. Am. Chem. Soc.* **2014**, *136*, 3803-3816.

(44) Tressler, C. M.; Zondlo, N. J. (2S,4R)- and (2S,4S)-Perfluoro-tert-butyl 4-Hydroxyproline: Two Conformationally Distinct Proline Amino Acids for Sensitive Application in 19F NMR. *J. Org. Chem.* **2014**, *79*, 5880-5886.

(45) Tressler, C. M.; Zondlo, N. J. Perfluoro-tert-butyl Homoserine is a Helix-Promoting, Highly Fluorinated, NMR-Sensitive Aliphatic Amino Acid: Detection of the Estrogen Receptor•Coactivator Protein-Protein Interaction by 19F NMR. *Biochemistry* **2017**, *56*, 1062-1074.

(46) Grundke-Iqbal, I.; Iqbal, K.; Tung, Y. C.; Quinlan, M.; Wisniewski, H. M.; Binder, L. I. Abnormal Phosphorylation of the Microtubule-Associated Protein-Tau (Tau) in Alzheimer Cytoskeletal Pathology. *Proc. Natl. Acad. Sci. U.S.A.* **1986**, *83*, 4913-4917.

(47) Otvos, L.; Feiner, L.; Lang, E.; Szendrei, G. I.; Goedert, M.; Lee, V. M. Y. Monoclonal-Antibody PHF-1 Recognizes Tau-Protein Phosphorylated at Serine Residue-396 and Residue-404. *J. Neurosci. Res.* **1994**, *39*, 669-673.

(48) Hong, M.; Zhukareva, V.; Vogelsberg-Ragaglia, V.; Wszolek, Z.; Reed, L.; Miller, B. I.; Geschwind, D. H.; Bird, T. D.; McKeel, D.; Goate, A.; Morris, J. C.; Wilhelmsen, K. C.; Schellenberg, G. D.; Trojanowski, J. Q.; Lee, V. M. Y. Mutation-specific functional impairments in distinct Tau isoforms of hereditary FTDP-17. *Science* **1998**, *282*, 1914-1917.

(49) Hasegawa, M.; Smith, M. J.; Goedert, M. Tau proteins with FTDP-17 mutations have a reduced ability to promote microtubule assembly. *FEBS Lett.* **1998**, *437*, 207-210.

(50) Perez, M.; Lim, F.; Arrasate, M.; Avila, J. The FTDP-17-linked mutation R406W abolishes the interaction of phosphorylated tau with microtubules. *J. Neurochem.* **2000**, *74*, 2583-2589.

(51) Barghorn, S.; Zheng-Fischhofer, Q.; Ackmann, M.; Biernat, J.; von Bergen, M.; Mandelkow, E. M.; Mandelkow, E. Structure, microtubule interactions, and paired helical filament aggregation by tau mutants of frontotemporal dementias. *Biochemistry* **2000**, *39*, 11714-11721.

(52) Tatebayashi, Y.; Miyasaka, T.; Chui, D. H.; Akagi, T.; Mishima, K.; Iwasaki, K.; Fujiwara, M.; Tanemura, K.; Murayama, M.; Ishiguro, K.; Planel, E.; Sato, S.; Hashikawa, T.; Takashima, A. Tau filament formation and associative memory deficit in aged mice expressing mutant (R406W) human tau. *Proc. Natl. Acad. Sci. U.S.A.* **2002**, *99*, 13896-13901.

(53) Cantrelle, F. X.; Loyens, A.; Trivelli, X.; Reimann, O.; Despres, C.; Gandhi, N. S.; Hackenberger, C. P. R.; Landrieu, I.; Smet-Nocca, C. Phosphorylation and O-GlcNAcylation of the PHF-1 Epitope of Tau Protein Induce Local Conformational Changes of the C-Terminus and Modulate Tau Self-Assembly Into Fibrillar Aggregates. *Front. Mol. Neurosci.* **2021**, *14*, 661368.

(54) Ganguly, H. K.; Elbaum, M. B.; Zondlo, N. J. Serine-404 Phosphorylation and the R406W Modification in Tau Stabilize the cis-Proline Amide Bond, via Phosphoserine-Proline C–H/O and Proline-Aromatic C–H/π Interactions. *chemRxiv* **2023**, DOI: 10.26434/chemrxiv-22023-26437nb26444.

(55) Milner-White, E. J.; Bell, L. H.; Maccallum, P. H. Pyrrolidine ring puckering in cis and trans-proline residues in proteins and polypeptides: Different puckers are favoured in certain situations. *J. Mol. Biol.* **1992**, *228*, 725-734.

(56) Lovell, S. C.; Word, J. M.; Richardson, J. S.; Richardson, D. C. The Penultimate Rotamer Library. *Proteins* **2000**, *40*, 389-408.

(57) Krimm, S. Hydrogen Bonding of C-H...O=C in Proteins. *Science* **1967**, *158*, 530-531.

(58) Gu, Y. L.; Kar, T.; Scheiner, S. Fundamental properties of the CH center dot center dot center dot O interaction: Is it a true hydrogen bond? *J. Am. Chem. Soc.* **1999**, *121*, 9411-9422.

(59) Jiang, L.; Lai, L. H. CH center dot center dot center dot O hydrogen bonds at protein-protein interfaces. *J. Biol. Chem.* **2002**, *277*, 37732-37740.

(60) Horowitz, S.; Trievel, R. C. Carbon-Oxygen Hydrogen Bonding in Biological Structure and Function. *J. Biol. Chem.* **2012**, *287*, 41576-41582.

(61) Krimm, S.; Kuroiwa, K. Low temperature imfrared spectra of polyglycines amd C-H...O=C hydrogen bonding in polyglycine II. *Biopolymers* **1968**, *6*, 401-407.

(62) Daniecki, N. J.; Bhatt, M. R.; Yap, G. P. A.; Zondlo, N. J. Proline C-H Bonds as Loci for Proline Assembly via C-H/O Interactions. *ChemBioChem* **2022**, *23*, e202200409.

(63) Improta, R.; Benzi, C.; Barone, V. Understanding the role of stereoelectronic effects in determining collagen stability. 1. A quantum mechanical study of proline, hydroxyproline, and fluoroproline dipeptide analogues in aqueous solution. *J. Am. Chem. Soc.* **2001**, *123*, 12568-12577.

(64) Vitagliano, L.; Berisio, R.; Mastrangelo, A.; Mazzarella, L.; Zagari, A. Preferred proline puckerings in cis and trans peptide groups: Implications for collagen stability. *Protein Sci.* **2001**, *10*, 2627-2632.

(65) DeRider, M. L.; Wilkens, S. J.; Waddell, M. J.; Bretscher, L. E.; Weinhold, F.; Raines, R. T.; Markley, J. L. Collagen Stability: Insights from NMR Spectroscopic and Hybrid Density Functional Computational Investigations of the Effect of Electronegative Substituents on Prolyl Ring Conformations. *J. Am. Chem. Soc.* **2002**, *124*, 2497-2505.

(66) Ho, B. K.; Coutsias, E. A.; Seok, C.; Dill, K. A. The flexibility in the proline ring couples to the protein backbone. *Protein Sci.* **2005**, *14*, 1011-1018.

(67) Schüler, M.; O'Hagan, D.; Slawin, A. M. Z. The vicinal F–C–C–F moiety as a tool for influencing peptide conformation. *Chem. Commun.* **2005**, 4324-4326.

(68) Dahanayake, J. N.; Kasireddy, C.; Karnes, J. P.; Verma, R.; Steinert, R. M.; Hildebrandt, D.; Hull, O. A.; Ellis, J. M.; Mitchell-Koch, K. R. Progress in Our Understanding of F-19 Chemical Shifts. *Annu. Rep. NMR Spectrosc.* **2018**, *93*, 281-365.

(69) Dahanayake, J. N.; Kasireddy, C.; Ellis, J. M.; Hildebrandt, D.; Hull, O. A.; Karnes, J. P.; Morlan, D.; Mitchell-Koch, K. R. Evaluating Electronic Structure Methods for Accurate Calculation of F-19 Chemical Shifts in Fluorinated Amino Acids. *J. Comput. Chem.* **2017**, *38*, 2605-2617.

(70) Thiehoff, C.; Rey, Y. P.; Gilmour, R. The Fluorine Gauche Effect: A Brief History. *Isr. J. Chem.* **2017**, *57*, 92-100.

(71) Juaristi, E.; Cuevas, G. Recent Studies of the Anomeric Effect. *Tetrahedron* **1992**, *48*, 5019-5087.

(72) Filloux, C. M. The Problem of Origins and Origins of the Problem: Influence of Language on Studies Concerning the Anomeric Effect. *Angew. Chem., Int. Ed.* **2015**, *54*, 8880-8894.

(73) Pandey, A. K.; Yap, G. P. A.; Zondlo, N. J. (2S,4R)-4-Hydroxyproline(4-Nitrobenzoate): Strong Induction of Stereoelectronic Effects via a Readily Synthesized Proline Derivative. Crystallographic Observation of a Correlation between Torsion Angle and Bond Length in a Hyperconjugative Interaction. *J. Org. Chem.* **2014**, *79*, 4174-4179.

(74) Durr, U. H. N.; Grage, S. L.; Witter, R.; Ulrich, A. S. Solid state F-19 NMR parameters of fluorine-labeled amino acids. Part I: Aromatic substituents. *J. Magn. Reson.* **2008**, *191*, 7-15.

(75) Grage, S. L.; Durr, U. H. N.; Afonin, S.; Mikhailiuk, P. K.; Komarov, I. V.; Ulrich, A. S. Solid state F-19 NMR parameters of fluorine-labeled amino acids. Part II: Aliphatic substituents. *J. Magn. Reson.* **2008**, *191*, 16-23.

(76) Fritz, M.; Kraus, J.; Quinn, C. M.; Yap, G. P. A.; Struppe, J.; Sergeyev, I. V.; Gronenborn, A. M.; Polenova, T. Measurement of Accurate Interfluorine Distances in Crystalline Organic Solids: A High-Frequency Magic Angle Spinning NMR Approach. *J. Phys. Chem. B* **2019**, *123*, 10680-10690.

(77) Shi, Z. S.; Woody, R. W.; Kallenbach, N. R. Is polyproline II a major backbone conformation in unfolded proteins? *Adv. Protein Chem.* **2002**, *62*, 163-240.

(78) Liu, Z. G.; Chen, K.; Ng, A.; Shi, Z. S.; Woody, R. W.; Kallenbach, N. R. Solvent dependence of PII conformation in model alanine peptides. *J. Am. Chem. Soc.* **2004**, *126*, 15141-15150.

(79) Mezei, M.; Fleming, P. J.; Srinivasan, R.; Rose, G. D. Polyproline II helix is the preferred conformation for unfolded polyalanine in water. *Proteins* **2004**, *55*, 502-507.

(80) Meral, D.; Toal, S.; Schweitzer-Stenner, R.; Urbanc, B. Water-Centered Interpretation of Intrinsic pPII Propensities of Amino Acid Residues: In Vitro-Driven Molecular Dynamics Study. *J. Phys. Chem. B* **2015**, *119*, 13237-13251.

(81) Zondlo, N. J. Solvation stabilizes intercarbonyl n→π* interactions and polyproline II helix. *Phys. Chem. Chem. Phys.* **2022**, *24*, 13571-13586.

(82) Lin, Y. J.; Chang, C. H.; Horng, J. C. The Impact of 4-Thiaproline on Polyproline Conformation. *J. Phys. Chem. B* **2014**, *118*, 10813-10820.

(83) Tiffany, M. L.; Krimm, S. Extended Conformations of Polypeptides and Proteins in Urea and Guanidine Hydrochloride. *Biopolymers* **1973**, *12*, 575-587.

(84) Whittington, S. J.; Chellgren, B. W.; Hermann, V. M.; Creamer, T. P. Urea promotes polyproline II helix formation: Implications for protein denatured states. *Biochemistry* **2005**, *44*, 6269-6275.

(85) Elam, W. A.; Schrank, T. P.; Campagnolo, A. J.; Hilser, V. J. Temperature and Urea Have Opposing Impacts on Polyproline II Conformational Bias. *Biochemistry* **2013**, *52*, 949-958.

(86) Bretscher, L. E.; Jenkins, C. L.; Taylor, K. M.; DeRider, M. L.; Raines, R. T. Conformational Stability of Collagen Relies on a Stereoelectronic Effect. *J. Am. Chem. Soc.* **2001**, *123*, 777-778.

(87) Hodges, J. A.; Raines, R. T. Stereoelectronic effects on Collagen Stability: The Dichotomy of 4-Fluoroproline Diastereomers. *J. Am. Chem. Soc.* **2003**, *125*, 9262-9263.

(88) Horng, J. C.; Raines, R. T. Stereoelectronic effects on polyproline conformation. *Protein Sci.* **2006**, *15*, 74-83.

(89) von Bergen, M.; Barghorn, S.; Li, L.; Marx, A.; Biernat, J.; Mandelkow, E. M.; Mandelkow, E. Mutations of tau protein in frontotemporal dementia promote aggregation of paired helical filaments by enhancing local beta-structure. *J. Biol. Chem.* **2001**, *276*, 48165-48174.

(90) Wang, J. Z.; Grundke-Iqbal, I.; Iqbal, K. Kinases and phosphatases and tau sites involved in Alzheimer neurofibrillary degeneration. *Eur. J. Neurosci.* **2007**, *25*, 59-68.

(91) Frost, B.; Ollesch, J.; Wille, H.; Diamond, M. I. Conformational Diversity of Wild-type Tau Fibrils Specified by Templated Conformation Change. *J. Biol. Chem.* **2009**, *284*, 3546-3551.

(92) MacArthur, M. W.; Thornton, J. M. Influence of proline residues on protein conformation. *J. Mol. Biol.* **1991**, *218*, 397-412.

(93) Schmid, F. X. Prolyl isomerases. *Adv. Protein Chem.* **2002**, *59*, 243-282.

(94) Andreotti, A. H. Native State Proline Isomerization: An Intrinsic Molecular Switch. *Biochemistry* **2003**, *42*, 9515-9524.

(95) Fischer, G. Peptidyl-prolyl cis/trans isomerases and their effectors. *Angew. Chem. Int. Ed.* **1994**, *33*, 1415-1436.

(96) Zondlo, N. J. Aromatic-Proline Interactions: Electronically Tunable CH/pi Interactions. *Acc. Chem. Res.* **2013**, *46*, 1039-1049.

(97) Agouridas, V.; El Mahdi, O.; Diemer, V.; Cargoet, M.; Monbaliu, J. C. M.; Melnyk, O. Native Chemical Ligation and Extended Methods: Mechanisms, Catalysis, Scope, and Limitations. *Chem. Rev.* **2019**, *119*, 7328-7443.

(98) Thompson, R. E.; Muir, T. W. Chemoenzymatic Semisynthesis of Proteins. *Chem. Rev.* **2020**, *120*, 3051-3126.

(99) Li, C. G.; Wang, G. F.; Wang, Y. Q.; Creager-Allen, R.; Lutz, E. A.; Scronce, H.; Slade, K. M.; Ruf, R. A. S.; Mehl, R. A.; Pielak, G. J. Protein (19)F NMR in Escherichia coli. *J. Am. Chem. Soc.* **2010**, *132*, 321-327.

(100) Veronesi, M.; Giacomina, F.; Romeo, E.; Castellani, B.; Ottonello, G.; Lambruschini, C.; Garau, G.; Scarpelli, R.; Bandiera, T.; Piomelli, D.; Dalvit, C. Fluorine nuclear magnetic resonance-based assay in living mammalian cells. *Anal. Biochem.* **2016**, *495*, 52-59.

(101) Tressler, C. M.; Zondlo, N. J. Perfluoro-tert-Butyl Hydroxyprolines as Sensitive, Conformationally Responsive Molecular Probes: Detection of Protein Kinase Activity by 19F NMR. *ACS Chem. Biol.* **2020**, *15*, ASAP.

(102) Habchi, J.; Tompa, P.; Longhi, S.; Uversky, V. N. Introducing Protein Intrinsic Disorder. *Chem. Rev.* **2014**, *114*, 6561-6588.

(103) Wright, P. E.; Dyson, H. J. Intrinsically disordered proteins in cellular signalling and regulation. *Nat. Rev. Mol. Cell. Biol.* **2015**, *16*, 18-29.

(104) Bah, A.; Forman-Kay, J. D. Modulation of Intrinsically Disordered Protein Function by Post-translational Modifications. *J. Biol. Chem.* **2016**, *291*, 6696-6705.

(105) Reiersen, H.; Rees, A. R. The hunchback and its neighbours: proline as an environmental modulator. *Trends Biochem. Sci.* **2001**, *26*, 679-684.

(106) Mateos, B.; Conrad-Billroth, C.; Schiavina, M.; Beier, A.; Kontaxis, G.; Konrat, R.; Felli, I. C.; Pierattelli, R. The Ambivalent Role of Proline Residues in an Intrinsically Disordered Protein: From Disorder Promoters to Compaction Facilitators. *J. Mol. Biol.* **2020**, *432*, 3093-3111.

(107) Gibbs, E. B.; Cook, E. C.; Showalter, S. A. Application of NMR to studies of intrinsically disordered proteins. *Arch. Biochem. Biophys.* **2017**, *628*, 57-70.

(108) Sebak, F.; Ecsedi, P.; Bermel, W.; Luy, B.; Nyitray, L.; Bodor, A. Selective H-1(alpha) NMR Methods Reveal Functionally Relevant Proline cis/trans Isomers in Intrinsically Disordered Proteins: Characterization of Minor Forms, Effects of Phosphorylation, and Occurrence in Proteome. *Angew. Chem., Int. Ed.* **2022**, *61*, e202108361.

(109) Frisch, M. J.; Trucks, G. W.; Schlegel, H. B.; Scuseria, G. E.; Robb, M. A.; Cheeseman, J. R.; Scalmani, G.; Barone, V.; Mennucci, B.; Petersson, G. A.; Nakatsuji, H.; Caricato, M.; Li, X.; Hratchian, H. P.; Izmaylov, A. F.; Bloino, J.; Zheng, G.; Sonnenberg, J. L.; Hada, M.; Ehara, M.; Toyota, K.; Fukuda, R.; Hasegawa, J.; Ishida, M.; Nakajima, T.; Honda, Y.; Kitao, O.; Nakai, H.; Vreven, T.; Montgomery, J., J. A.; Peralta, J. E.; Ogliaro, F.; Bearpark, M.; Heyd, J. J.; Brothers, E.; Kudin, K. N.; Staroverov, V. N.; Keith, T.; Kobayashi, R.; Normand, J.; Raghavachari, K.; Rendell, A.; Burant, J. C.; Iyengar, S. S.; Tomasi, J.; Cossi, M.; Rega, N.; Millam, J. M.; Klene, M.; Knox, J. E.; Cross, J. B.; Bakken, V.; Adamo, C.; Jaramillo, J.; Gomperts, R.; Stratmann, R. E.; Yazyev, O.; Austin, A. J.; Cammi, R.; Pomelli, C.; Ochterski, J. W.; Martin, R. L.; Morokuma, K.; Zakrzewski, V. G.; Voth, G. A.; Salvador, P.; Dannenberg, J. J.; Dapprich, S.; Daniels, A. D.; Farkas, O.; Foresman, J. B.; Ortiz, J. V.; Cioslowski, J.; Fox, D. J.: Gaussian 09, Revision D.01. Gaussian, Inc.: Wallingford, CT, 2013.

(110) Zhao, Y.; Truhlar, D. G. The M06 suite of density functionals for main group thermochemistry, thermochemical kinetics, noncovalent interactions, excited states, and transition elements: two new functionals and systematic testing of four M06-class functionals and 12 other functionals. *Theor. Chem. Acc.* **2008**, *120*, 215-241.

(111) Raghavachari, K.; Binkley, J. S.; Seeger, R.; Pople, J. A. Self-Consistent Molecular Orbital Methods. 20. Basis sets for correlated wave functions. *J. Chem. Phys.* **1980**, *72*, 650-654.

(112) Tomasi, J.; Mennucci, B.; Cances, E. The IEF version of the PCM solvation method: an overview of a new method addressed to study molecular solutes at the QM ab initio level. *J. Mol. Struct. THEOCHEM* **1999**, *464*, 211-226.

(113) Wolinski, K.; Hinton, J. F.; Pulay, P. Efficient Implementation of the Gauge-Independent Atomic Orbital Method for Nmr Chemical-Shift Calculations. *J. Am. Chem. Soc.* **1990**, *112*, 8251-8260.

(114) Cheeseman, J. R.; Trucks, G. W.; Keith, T. A.; Frisch, M. J. A comparison of models for calculating nuclear magnetic resonance shielding tensors. *J. Chem. Phys.* **1996**, *104*, 5497-5509.

Graphical Table of Contents